FORUM REVIEW ARTICLE

Bacterial Mechanosensitive Channels: Models for Studying Mechanosensory Transduction

Boris Martinac,[1,2] Takeshi Nomura,[1] Gamma Chi,[3] Evgeny Petrov,[1] Paul R. Rohde,[1] Andrew R. Battle,[4,5] Alexander Foo,[3] Maryrose Constantine,[1] Rosalba Rothnagel,[3] Sonia Carne,[5] Evelyne Deplazes,[3] Bruce Cornell,[5] Charles G. Cranfield,[1,2] Ben Hankamer,[3] and Michael J. Landsberg[3]

Abstract

Significance: Sensations of touch and hearing are manifestations of mechanical contact and air pressure acting on touch receptors and hair cells of the inner ear, respectively. In bacteria, osmotic pressure exerts a significant mechanical force on their cellular membrane. Bacteria have evolved mechanosensitive (MS) channels to cope with excessive turgor pressure resulting from a hypo-osmotic shock. MS channel opening allows the expulsion of osmolytes and water, thereby restoring normal cellular turgor and preventing cell lysis. *Recent Advances:* As biological force-sensing systems, MS channels have been identified as the best examples of membrane proteins coupling molecular dynamics to cellular mechanics. The bacterial MS channel of large conductance (MscL) and MS channel of small conductance (MscS) have been subjected to extensive biophysical, biochemical, genetic, and structural analyses. These studies have established MscL and MscS as model systems for mechanosensory transduction. *Critical Issues:* In recent years, MS ion channels in mammalian cells have moved into focus of mechanotransduction research, accompanied by an increased awareness of the role they may play in the pathophysiology of diseases, including cardiac hypertrophy, muscular dystrophy, or Xerocytosis. *Future Directions:* A recent exciting development includes the molecular identification of Piezo proteins, which function as nonselective cation channels in mechanosensory transduction associated with senses of touch and pain. Since research on Piezo channels is very young, applying lessons learned from studies of bacterial MS channels to establishing the mechanism by which the Piezo channels are mechanically activated remains one of the future challenges toward a better understanding of the role that MS channels play in mechanobiology. *Antioxid. Redox Signal.* 00, 000–000.

Introduction

ION CHANNELS FUNCTION as molecular pores in the membranes of living cells. Since cellular membranes are impermeable boundaries for hydrophilic ionized solutes, separating the cell interior from the extracellular space, the main role of ion channels is to facilitate permeation of physiologically important ions, including calcium, chloride, potassium, and sodium ions across cell membranes. Ionic currents flowing through these channels in and out of the cells generate electrical signals that cause cascades of intracellular events underlying biological processes such as sensory transduction in senses of sight, smell, touch, taste and vision, muscle movement, and heartbeat as well as secretion of hormones and gastric acid.

The existence of ion channels in neuronal membranes was postulated by Alan Hodgkin and Andrew Huxley in the early 1950s, based on their electrophysiological experiments performed in the squid giant axon (62–64, 66). Since that time, a substantial number of studies have focused on ion channels from animal and human cells. Over the last 20 years, however, a large diversity of ion channels has also been found in the

---

[1]Molecular Cardiology and Biophysics Division/Mechanosensory Biophysics Laboratory, Victor Chang Cardiac Research Institute, Darlinghurst, Australia.
[2]St. Vincent's Clinical School, University of New South Wales, Kensington, Australia.
[3]Division of Chemistry and Structural Biology, Institute for Molecular Bioscience, The University of Queensland, St. Lucia, Australia.
[4]School of Pharmacy and Griffith Health Institute, Griffith University, Parklands, Australia.
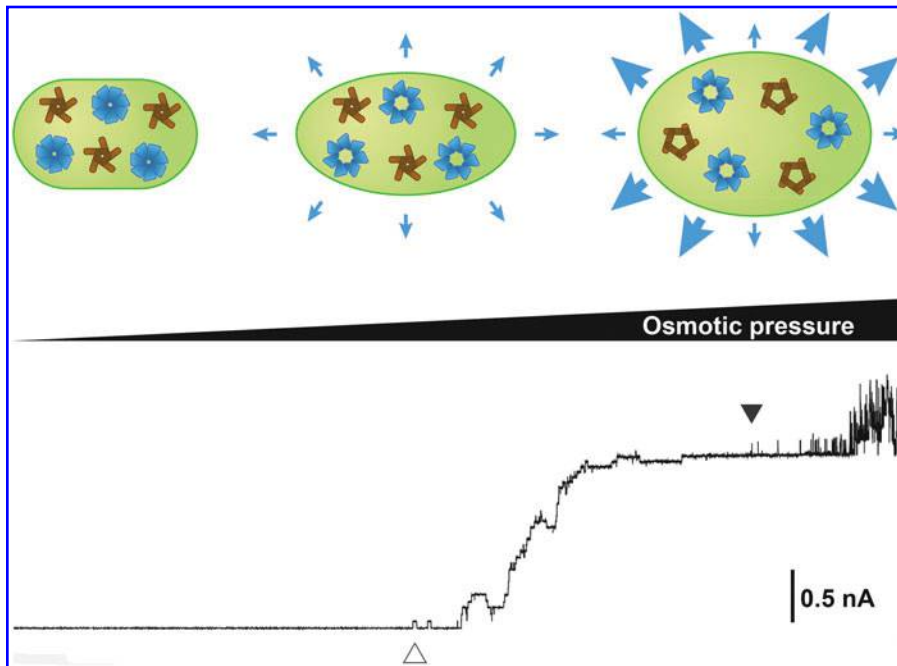[5]Surgical Diagnostics Pty Ltd., St. Roseville, Australia.

FIG. 1. Activation of MS channels in response to osmotic shock. A schematic representation of the role of MscS and MscL in bacteria. In a weakly hyposmotic environment, MscS channels are gated to alleviate osmotic stress. In an environment with much higher osmotic pressure, MscL in addition to MscS also opens for a more rapid discharge of intracellular contents. A typical patch-clamp trace shows the points at which first MscS (*open triangle*) and subsequently MscL channels (*closed triangle*) are gated in response to an applied, increasing gradient of transmembrane tension. MS, mechanosensitive; MscL, mechanosensitive channel of large conductance; MscS, mechanosensitive channel of small conductance. To see this illustration in color, the reader is referred to the web version of this article at www.liebertpub.com/ars

membranes of prokaryotic cells (Bacteria, Archaea). Paradoxically, much of what is known of the structure of eukaryotic ion channels is based on the structure of bacterial channels. This is largely due to the simpler structure of prokaryotic ion channels and the better suitability of bacterial cells for study in a laboratory environment (79). Bacteria also contain a substantial variety of mechanosensitive (MS) ion channel species, which has led to the identification of a further class of ion channel functionality, in addition to voltage-gated and ligand-gated ion channels (93).

The direct observation of ion channel function was revolutionized through the development of the patch-clamp recording technique by Erwin Neher and Bert Sakmann (56), which allowed electrophysiologists to measure the transmembrane currents from eukaryotic cells. However, the small size of bacterial cells presents major challenges for the direct application of a patch-clamp pipette to bacteria. An essential alternative to patching bacteria has been the use of a specific type of bacterial preparation named "giant spheroplasts" that allowed the problem of small size to be circumvented and, thus, enabled the recording of ion-channel activities in the bacterial cell membrane (95). The patch-clamp technique made possible the discovery of MS channels in bacteria.

As biological force-sensing systems activated by cell membrane deformation, MS ion channels present the best example of coupling molecular dynamics (MD) of membrane proteins to the mechanics of the surrounding cell membrane (83, 93). They are currently considered the major mechanosensors transducing mechanical stimuli exerted on membranes of living cells into electrical or chemical intracellular signals, and are, to date, among the most firmly established biological mechanosensors (23, 48, 55). In addition to lipid bilayer tension as an activator of MS channels, they may also be activated by forces induced *via* cytoskeletal and/or extracellular matrix linkages (13, 23).

The mechanical energy necessary for activation of MS channels corresponds to the free energy difference between at least two basic conformational states which MS channels can adopt, that is, the closed and the open state. This energy is defined by the following expression:

$$\Delta G = T\,(A_0 - A_c) = T\Delta A \quad (1),$$

where T is the membrane tension (expressed in mNm^{-1}) opening the MS channels and A_o and A_c are areas of the open and closed channels, respectively (133). The larger the difference in area, ΔA, the more likely membrane tension is the primary stimulus gating the channel; that is, the channel is considered genuinely mechanically gated (MS) rather than just being modulated by membrane tension as a secondary stimulus. In general, an ion channel can be considered being MS if the radius of the channel protein increases by at least 0.1–0.2 nm when open, as in the case of the mammalian 2-P type potassium-specific TREK-1 MS channel (92, 133).

MS channels have a fundamental function in sensory physiological processes such as touch, hearing, fluid balance, and blood pressure regulation. Diseases associated with malfunction of these channels include cardiac hypertrophy and arrhythmias, muscular dystrophy, Xerocytosis, neuronal degeneration, and pathological pain (9, 49, 159, 168). In bacteria, these channels function as safety valves protecting bacterial cells challenged by osmotic forces (Fig. 1). Bacterial MS channels have been particularly significant as a paradigm for research into the mechanical coupling of the lipid bilayer mechanics to MS channel activation (93). However, despite a wealth of structural and biochemical studies that are aimed at elucidating the conformational changes involved in the opening of the bacterial MS channels, a clear understanding of how forces transmitted from the surrounding lipid bilayer activate these proteins still remains elusive (81, 93). In this review, we summarize more than two decades of research on bacterial MS channels. Starting with the discovery of bacterial MS channels in 1987, the review describes major aspects of this research, including cloning of the mechanosensitive
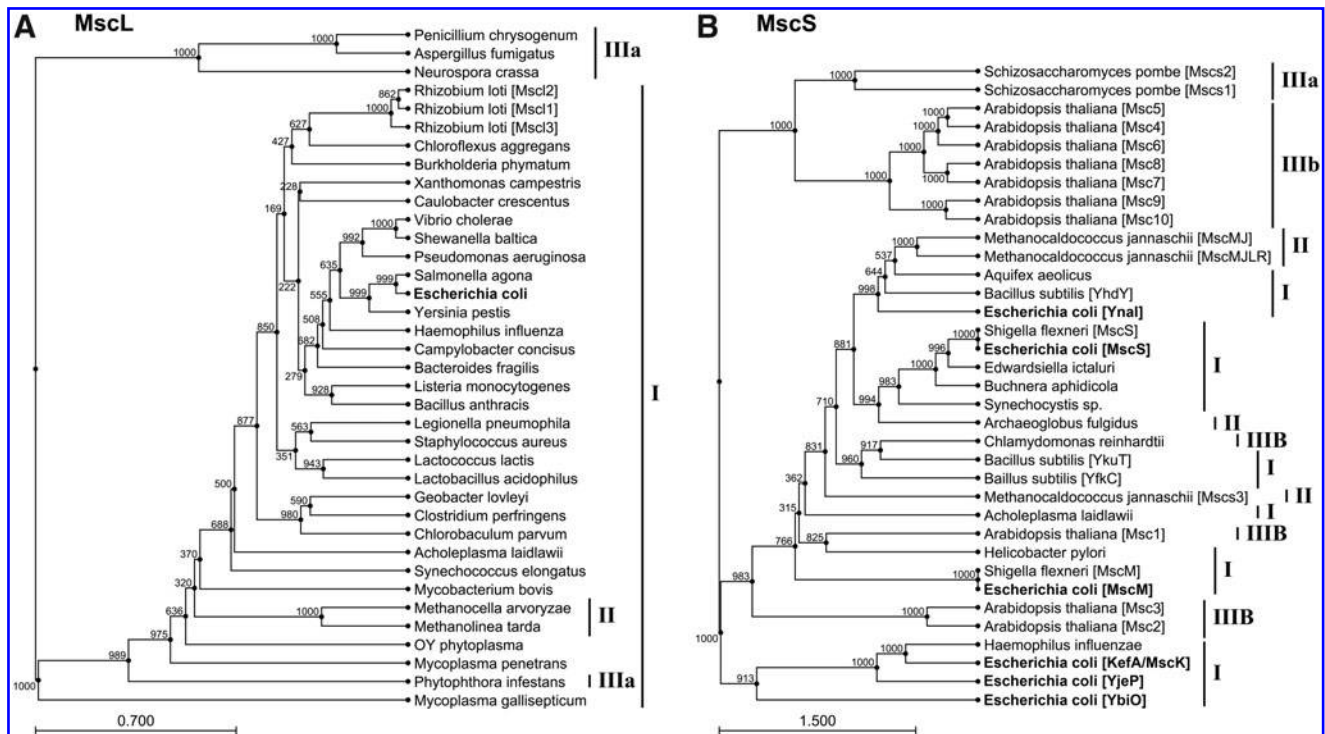
FIG. 2. **MscL and MscS families of prokaryotic MS channels.** A reduced phylogenetic tree showing the distribution of MscL and MscS, homologues of which are found across all three domains of life. **(A)** MscL homologues are found in cell-walled and wall-less bacteria (I), Archaea (II), and fungi and oomycetes (belonging to the domain eukaryota, IIIa). Note that in this alignment the Archaea and oomycetes cluster with the cell wall-less bacteria (mycoplasma/phytoplasma/acholeplasma). **(B)** MscS homologues have additionally been identified in plants and unicellular green algae (IIIb) with multiple MscS homologues often found in a single organism. The different MscS homologues in *Escherichia coli* are in bold typeface to highlight the presence of at least three distinct clusters—MscS-like, MscM-like, and MscK-like—suggesting that the acquisition of multiple MscS-like homologues appears to have occurred, at least for some homologues, at a much earlier evolutionary time point than the rare cases in which this has occurred for MscL (*e.g., Rhizobium loti*). Phylogenetic trees were constructed using 1000 bootstrapped iterations of the UPGMA algorithm in CLC Sequence Viewer (CLC bio, Aarhus Denmark). Scale bar indicates substitutions per site. For simplicity, organisms that contain multiple, uncharacterized MscS-like proteins have had them sequentially designated Mscs*N*, where *N* begins with the number of characterized homologues plus one and increments. *M. jannaschii* Mscs3 = Uniprot ID Q58111; *Schizosaccharomyces pombe* Mscs1 = O74839; *S. pombe* Mscs2 = O14050.

channel of large conductance (MscL) and mechanosensitive channel of small conductance (MscS) channels, determination of their three-dimensional (3D) crystal structure, spectroscopic and computational studies of their structural dynamics, as well as their prospective applications in research, medicine, and nanotechnology.

MS Channels Found in Bacteria

Since the first report on the discovery of MS channels in bacteria (95), multiple types of MS channels have been identified in *Escherichia coli* (44). Based on their primary structures, they can be separated into two different subfamilies—the MscL subfamily and the MscS subfamily. MscL and MscS are the only MS channels for which a physiological function can be clearly correlated with their structural and electrophysiological properties. Bacteria exposed to distilled water (osmotic downshock) rapidly release cytoplasmic contents into the surrounding medium *via* MscL and MscS, indicating that their function is as osmotically activated emergency valves (Fig. 1) (86).

Sequence alignments of MscL and MscS homologues from numerous bacteria and archaea (Fig. 2A, B) have revealed that

these two subfamilies of prokaryotic MS channels most likely evolved independently (115, 126). The UniProt database currently lists 2296 members of the MscL subfamily, with homologues identified in Gram-negative and Gram-positive bacteria as well as phytoplasma and mycoplasma that are specialized cell-wall deficient bacteria (65). Despite being widely represented, MscL is not ubiquitous across bacteria and is notably absent from many (but not all) bacteria that are native to marine environments. Representatives from MscL homologues have additionally been identified in numerous fungi (*e.g., Neurospora*), fungus-like organisms (*Phytophthora*), and Archaea (*e.g., Methanosarcina*) (65, 80, 96, 126). Thus, examples of MscL exist in three domains of life. Most MscL-containing organisms contain only a single homologue and in the few organisms in which multiple homologues have been identified (*e.g., Prevotella dentalis, Mesorhizobium loti*), these appear to have arisen from relatively recent gene duplication events. Residues of the MscL pore-forming transmembrane helix TM1 and the lipid bilayer-facing helix TM2 are highly conserved across all homologues.

Compared with the MscL subfamily, the MscS subfamily is more diverse and is represented not only in Bacteria, Archaea,
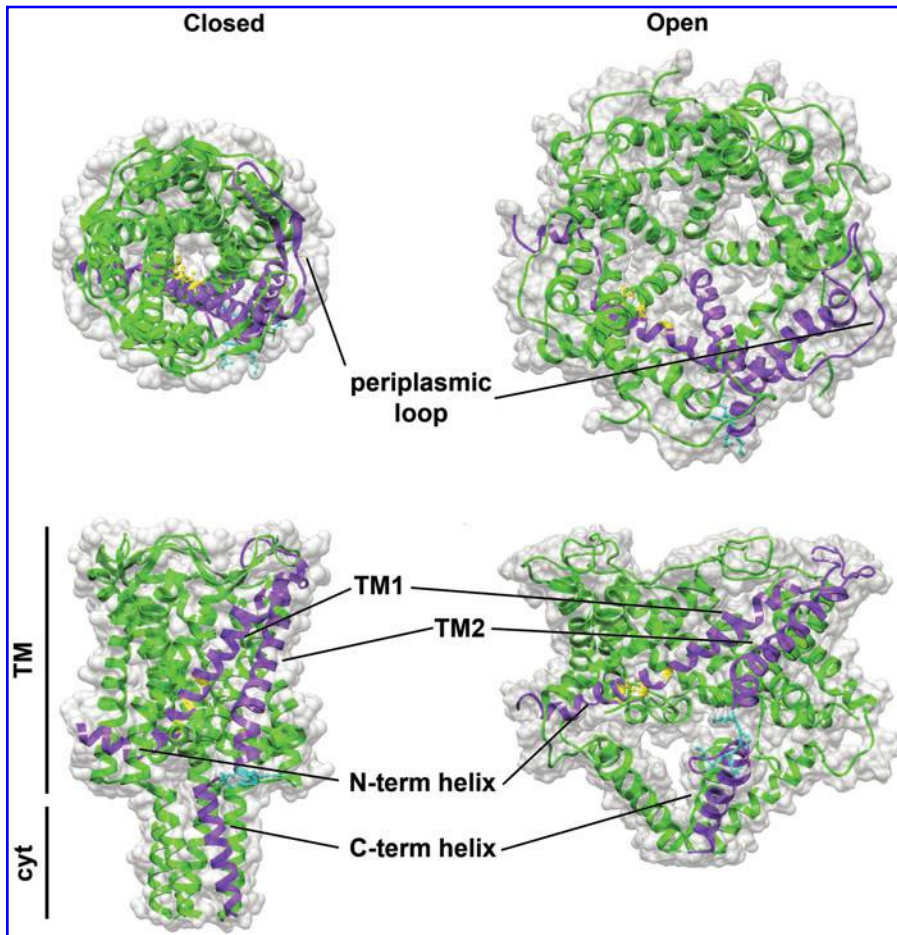
FIG. 3. Three-dimensional structure of MscL. Closed structure of *Mycobacterium tuberculosis* MscL and an open channel model of *E. coli* MscL viewed from the periplasmic side (*top*) and perpendicular to the plane of the membrane (*bottom*). A single subunit in each structure is colored purple to highlight the monomer. (TM, transmembrane domain; cyt, cytoplasmic domain). Conserved hydrophobic residues forming the pore constriction are highlighted yellow—L17/L19, V21/V23, and T25/A27 in *M. tuberculosis* and *E. coli* MscL, respectively. The pH-sensing RKK(G/E)E motif toward the bottom of TM2 is highlighted in cyan, while the transmembrane helices TM1 and TM2, the N- and C-terminal helices, and the periplasmic loop are additionally identified. To see this illustration in color, the reader is referred to the web version of this article at www.liebertpub.com/ars

and Fungi, but also in fission yeast (*Schizosaccaromyces*), a unicellular green alga (*Chlamydomonas*), and higher plants (60, 76, 96, 105, 126). Neither MscL nor MscS homologues have been identified in animal and human cells to date. While MscL is found in a number of cell wall-less mycoplasma and phytoplasma, so far, only a single MscS homologue has been found in such species, and that in *Acholeplasma laidlawii* (65). An additional difference between MscL and MscS is the typical presence of multiple MscS homologues within an organism, with as many as 10 identified in a single organism, as is the case for *Arabidopsis thaliana* (60). In *E. coli*, at least six MscS homologues exist: the canonical MscS, the subsequently identified MscK (potassium-dependent MS channel; originally KefA), MscM (MS channel of miniconductance; originally YbdG), and a further three MscS homologues, which have recently been characterized by electrophysiology and functional analyses (YjeP, YbiO, and YnaI) (44). Current evidence suggests that MscK-like homologues are restricted to Gram-negative bacteria. The different members of the MscS-like channel family share a conserved pore-forming transmembrane helix (TM3 in the original MscS) and a stretch of amino acids immediately after the C-terminal to TM3, which form the cytoplasmic beta domain in the MscS crystal structure (65).

Structure and Function of MscL and MscS

Structure of MscL

MscL is a homopentameric protein of 80 kDa (138). The structure of *Mycobacterium tuberculosis* MscL in a closed state

determined by Chang *et al.* in 1998 (24) and refined by Steinbacher *et al.* in 2007 (138, 139) consists of two transmembrane helices TM1 and TM2, N- and C-terminal domains located at the cytoplasmic side and a flexible loop connecting the two helices at the periplasmic side of the bacterial cell membrane. Each subunit has two transmembrane (TM1 and TM2) helices followed by one cytoplasmic C-terminal helix forming a structure resembling a stack of two cylinders (Fig. 3). In the transmembrane domain, TM1 largely forms the pore interface, while the TM2 helix dominates the lipid bilayer-facing surface. The N-terminal portion of the TM1 helix forms the constriction of the pore, with L19, V23, and A27 in *E. coli* (L17, V21 and T25 in *M. tuberculosis*) lining the constriction (141). The region around these residues also forms a part of the inter-subunit interface, while mutation of the smaller hydrophobic residues within this transmembrane domain results in enhanced sensitivity to membrane tension (5, 119). The pore closure is exposed on the periplasmic side, while on the cytoplasmic side, the pore is shielded by the five C-terminal helices (24, 114). The pore region of MscL lacks any charged residues for imparting an ion selectivity filter function and, by opening a pore of ∼30 Å in diameter, expands to such a degree that ion selection becomes impossible in the open state, rendering the channel nonselective (31, 38, 61, 121). This lack of ion selectivity in MscL and the large size of its open pore are essential for allowing passage of large organic osmolytes of ∼1000 in molecular weight and, hence, fulfilling its physiological role as a highly efficient emergency valve to release solutes from bacterial cells under

hypo-osmotic shock (82, 86). Although the structure of MscL in the fully open state has not yet been determined by X-ray crystallography, electronparamagnetic resonance (EPR) and Förster resonance energy transfer (FRET) spectroscopic studies employing the amphipath lysophosphatidylcholine (LPC) to open the channel in liposomes (31, 33, 123), as well as computational modelling (29, 31, 40, 52, 88, 121, 141, 146) have led to a general consensus on the structural dynamics of its transmembrane domains. According to all open-state models, the interaction between TM1 and TM2 does not significantly change from the closed to the open state, but the tilt angle of the subunits with regard to the membrane plane is increased by around 20° between the two channel conformations (31). All open channel models have a similar pore diameter of ~30 Å corresponding to the ~20 nm^2 in-plane protein expansion (28, 31, 40, 88, 121). A more recently solved structure of a partially open, tetrameric form of *Staphylococcus aureus* MscL (lacking its C-terminal cytoplasmic domain) supports these models (89). While the structure has been called into question by the subsequent finding that wild-type *S. aureus* MscL is pentameric (42), it is, nevertheless, worth noting that the structure, which features two antiparallel helices tilted at ~50° corresponding to the reorganization of the TM1 and TM2 domains, is characterized by a reduction in the height of the membrane spanning domain and the opening of a channel pore of ~30 Å in diameter. These data show good agreement with an earlier, electrophysiological, molecular sieving study carried out by Cruickshank *et al.* in 1997 (38) and a 2010 FRET study by Corry *et al.* (31) and suggest that structural plasticity is an inherent property of MscL.

The cytoplasmic domain starts at the end of the TM2 helix, where the RKKEE motif in MscL of *E. coli* (RKKGE in *M. tuberculosis*), critical for pH sensing and channel function, is located (57, 73). Reinterpretation of the crystal structure originally published by Chang *et al.* (24) revealed that the cytoplasmic C-terminal helices form a five-helix bundle (138) postulated by Anishkin and co-workers (6), where the hydrophobic residues are oriented inward (and not outward, as was incorrectly modeled in the original X-ray structure) in agreement with the EPR spectroscopic study of the closed form of MscL (122). Consequently, the inverted model of the C-terminal domain was adopted in the reinterpreted crystal structure (139). The cytoplasmic C-terminal helix is the least conserved area of MscL across species (10), and is reportedly nonessential for channel gating (1). Electron microscopy studies, along with the observed ability of MscL to let molecules as large as insulin pass through the pore, suggest that the C-terminal domain might dissociate and incorporate into the transmembrane domain during channel opening (151, 167). At odds with this, however, are MD simulations and mutational analyses, which suggest that the C-terminal domain remains intact and undergoes only minor dissociation proximal to the TM2 helix (31, 40, 52, 146, 162).

In contrast, the N-terminal domain appears to be very important for MscL function. Its 3D structure, unable to be modeled in the first MscL crystal structure reported (24), was revealed in the reinterpreted structure as a single α-helix (139). Several functional studies have demonstrated that even small N-terminal deletions or changes to the N-terminal amino-acid sequence are poorly tolerated, resulting in nonfunctional channels or channels which exhibit altered pressure sensitivity (20, 59, 143). More recent results suggest that the N-terminus

contributes to MscL mechanosensitivity by directly sensing membrane tension and transferring it to the pore lining helices, most likely by maintaining its position along the membrane–cytoplasm interface (31, 68). Here, the N-terminal domain functions as an anchor, guiding the TM1 transmembrane helix to a greater tilt during MscL opening (67).

The structure of the periplasmic loop, which connects the TM1 and TM2 helices of MscL, is not well defined. Its function is also not known, although it has been proposed that the loop behaves as a molecular spring, resisting the channel opening (1). This notion has found support from results of mutagenesis (100), EPR spectroscopic (102, 149), and MD studies (40, 103). Nevertheless, further experimental and modeling studies are needed to fully establish the role of this structural domain of MscL.

Structure of MscS

MscS is a larger, homoheptameric protein of 211 kDa (11). MscS has a more complex architecture than MscL, with three distinctive domains present: a transmembrane domain consisting of three α-helices, an intermediate cytoplasmic domain composed exclusively of β-strands, and a C-terminal cytoplasmic domain with a mix of helices and strands (Fig. 4) (11, 138). Similar to MscL, the transmembrane pore of MscS is exposed on the periplasmic side and constricted on the cytoplasmic side by residues L105 and L109 within the third transmembrane helix (11). The pore has been shown to open to ~16 Å on channel activation (140), which is smaller than the MscL open pore. Diffusion across this channel is further controlled by seven ~14 Å vestibular portals within the cytoplasmic domains (11, 47). Notably, both the closed and an expanded state structure of MscS show little change in the cytoplasmic domains (11, 155), and it has been postulated that in the fully conducting state the structure of this domain could remain unchanged (47).

Similar to MscL, the structural mechanism of MscS channel opening has not been conclusively determined so far. The two available structures, along with several mutational studies, have led to a view that hydrophobic residues facing the phospholipid bilayer act as the sensors for membrane tension (11, 15, 155), driving the tilt of transmembrane helices along the membrane and consequently opening the pore. Despite the availability of several models of MscS in expanded conformations (4, 7, 8, 27, 153, 155), a model of the fully open channel remains elusive and hence more experimental, and simulation studies are required to fully understand the mechanism of MscS gating by mechanical forces within the lipid bilayer.

Similar to MscL, MscS also serves as a safety valve that opens on a membrane stretch to release cytoplasmic osmolytes, relieving the excessive turgor pressure and preventing bacterial cell swelling and membrane damage (82, 86). However, MscS requires less tension for opening compared with MscL (65, 110, 144), allowing bacterial cells to respond in a graded manner to hypo-osmotic challenges (16). Unlike MscL, which has no preference for any ions, MscS exhibits a weak preference for anions compared with cations (43, 95, 140). This weak ion selectivity has recently been shown to originate from the charged residues within seven vestibular portals in the MscS cytoplasmic chamber, which is interesting, because, unlike voltage-gated K$^+$, Na$^+$ and Ca^{2+} channels, the selectivity of MscS is not determined by charged residues in the
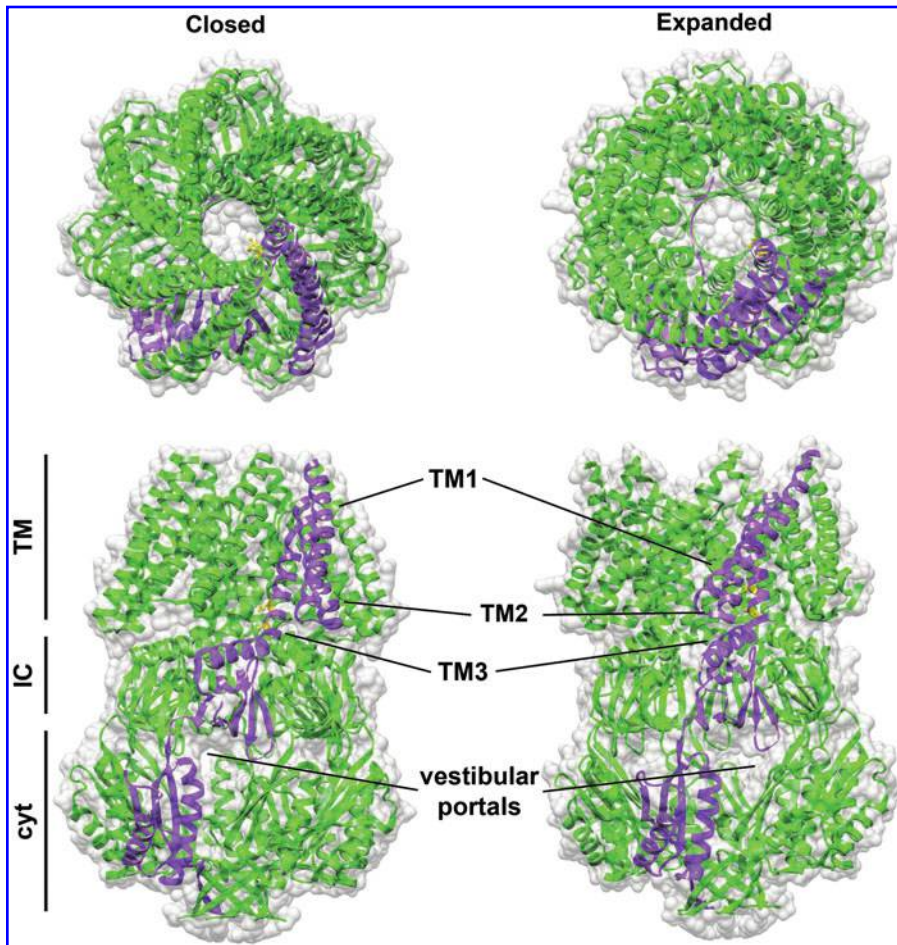
FIG. 4. Three-dimensional structure of MscS. Closed channel and an expanded channel structures of *E. coli* MscS viewed from the periplasmic side (*top*) and perpendicular to the plane of the membrane (*bottom*). A single subunit in each structure is colored purple to highlight the monomer. Subdomains are demarcated on the side-view closed conformations of both structures. (TM, transmembrane domain; IC, intermediate cytoplasmic domain; cyt, cytoplasmic domain). The conserved hydrophobic residues forming the pore constriction are highlighted yellow—L105 and L109 in *E. coli* MscS. TM1, TM2, and TM3 are identified along with the location of vestibular portals observed in the cytoplasmic domain of both MscS structures. To see this illustration in color, the reader is referred to the web version of this article at www.liebertpub.com/ars

channel pore but by residues outside the pore in the water-filled cytoplasmic domain (36, 47, 170).

MscL and MscS as a paradigm for mechanosensory transduction

Extensive multidisciplinary studies of MscL and MscS over the last 25 years have helped unravel the basic physical principles of MS channel gating by membrane tension (93). First, these studies unambiguously demonstrated that mechanical force gating of both channels originated purely from changes in the transbilayer pressure profile. This finding suggested that other types of MS channels could also be gated by the "bilayer mechanism" without the requirement for any other cellular components such as the cytoskeleton or extracellular matrix. The criterion for the "bilayer mechanism" is demonstration that the purified MS channel protein remains MS when reconstituted into lipid bilayers (57). In practical terms, this means that the sensitivity of the channel to lipid bilayer tension can be demonstrated on reconstitution into liposomes (99). Bacterial and archaeal MS channels provide a clear demonstration that prokaryotic MS channels can sense membrane tension directly. The tension develops in the lipid bilayer alone and directly gates these channels (57, 94). This has also been demonstrated for several eukaryotic MS channels (102).

Among the basic physical principles, hydrophobic mismatch is one of the global determinants of MscL channel conformations in the lipid bilayer, with thinner bilayers fa-

voring MscL opening compared with thicker bilayers. Interestingly, hydrophobic mismatch does not seem to play as significant a role in MscS gating (109). The other global determinant, bilayer curvature and/or transbilayer pressure profile, has been established as the major factor regulating MscL and MscS structural conformations. With regard to specific interactions of the MscL and MscS structural components with surrounding phospholipids, several studies have suggested that the periplasmic and cytoplasmic regions are critical for these interactions (103, 111, 149, 163, 166).

In order to establish the general physical principles underlying the biophysics of MS channel mechanosensitivity, future studies will be required to validate the key hypothesis of mechanical force being delivered through the lipid bilayer to MS ion channels in cells of different evolutionary origins. By using MscL and MscS as models, these studies could contribute to understanding the central question of how MS channels of different transmembrane architectures transduce mechanical stimuli into protein structural changes.

Techiques Used for Studies of Bacterial MS Channels

Studies of bacterial MS channels in giant spheroplasts of E. coli

The minute size of bacteria is prohibitive for direct application of the patch-clamp technique to a bacterial cell. The technique typically requires a larger bacterial object for recording
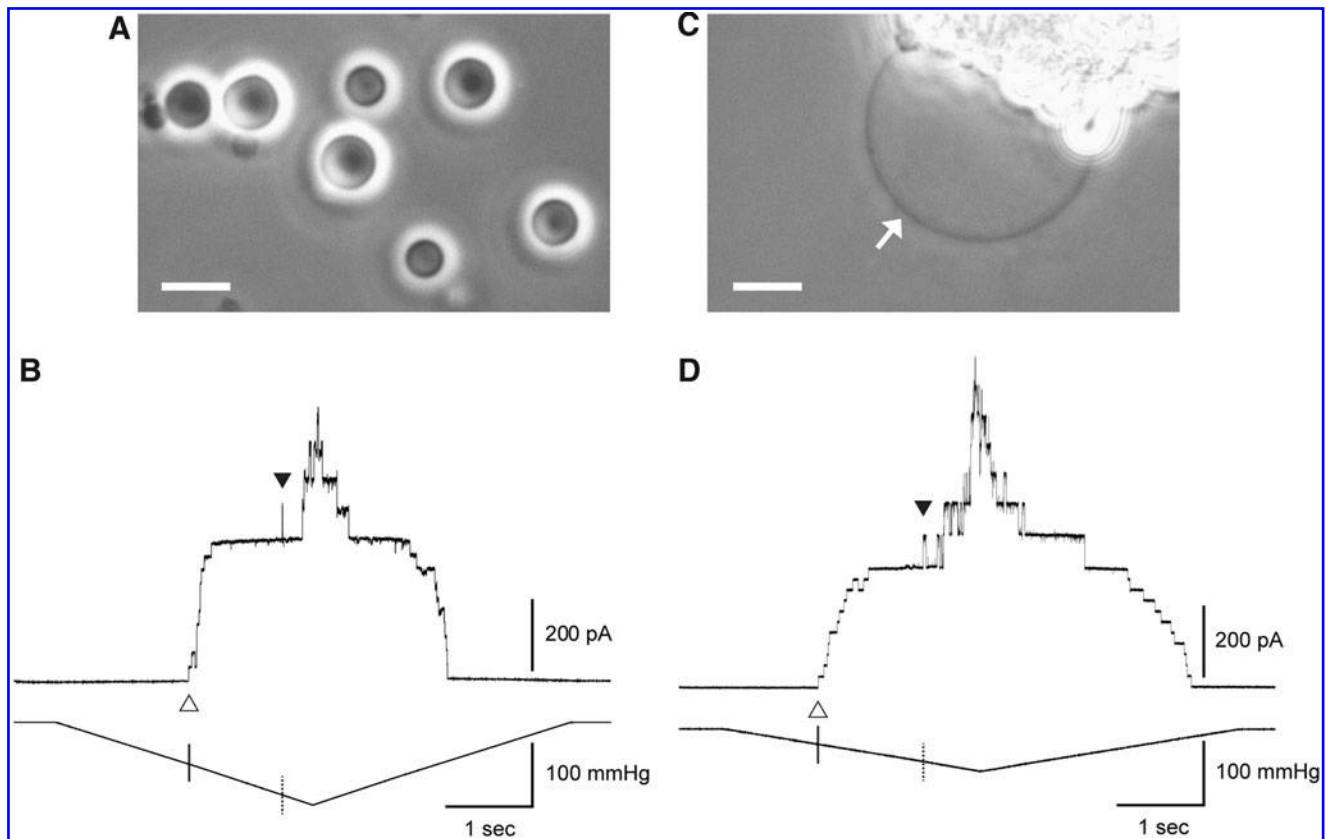
FIG. 5. Patch-clamp recording of MscL and MscS. Representative phase-contrast micrograph of *E. coli* giant spheroplasts **(A)** and azolectin (100%) liposomes (*arrow*) **(B)**. The scale bar shows 10 μm. Channel activities of MscS and MscL in spheroplasts (AW737) **(C)** and azolectin (100%) liposomes **(D)**. *Open and filled arrow heads* indicate the activation threshold of MscS and MscL, respectively. *Solid and dotted lines* show the pressure of the first opening of MscS and MscL. The activation thresholds of MscS and MscL were -62.4 and -108.3 mmHg in spheroplasts and -26.7 and -54.2 mmHg in azolectin (100%) liposomes, respectively. The threshold ratio (MscL/MscS) was 1.74 in spheroplasts and 2.03 in azolectin (100%) liposomes, respectively.

ion channel activities from the bacterial cell membrane. Development of the "giant spheroplast" preparation from *E. coli* cells (Fig. 5A) allowed for the first time electro-physiological studies in bacterial cell membranes (95, 132) and, thus, opened the way for pioneering structure and function studies of ion channel proteins in prokaryotic microbes (99).

For MS channel recording from giant spheroplast preparations, cell cultures of *E. coli* are grown in Luria–Bertani medium in the presence of cephalexin, which causes the cells to grow into filaments reaching a length of 50 to 150 μm. In the presence of lysozyme and ethylenediaminetetraacetic acid (EDTA), required for hydrolysis of the peptidoglycan layer, these bacterial filaments are converted into giant spheroplasts of 5 to 10 μm in diameter, which are then amenable to patch clamp recording (95, 98). Electrophysiological recording of ion currents arising from activation of MS channels is then achieved by applying voltage and negative pipette pressure (suction) to patch pipettes (Fig. 5B).

Reconstitution of MscL and MscS channels into liposomes

Instead of patching MS channels in spheroplasts, it is often desirable to do so using artificial lipid membranes. Subse-

quently, bacterial MS channel reconstitution into liposomes has become the gold standard for patch-clamp electrophysiology experiments, especially for MscL, where channel activity can be recorded in liposomes at protein/lipid ratios as low as 1:10,000 w/w (Fig. 5C) (97). Other prokaryotic MS channel proteins also successfully incorporated into liposomes using this method include those of the Archaeon *Haloferax volcanii* (85), the MscMJ and MscMJLR channels from *Methanococcus jannashii* (74, 75), as well as the MscSP channel from *Silicibacter pomeroyi* (124).

MscS has proved more difficult to incorporate into azolectin liposomes with much higher reconstitution ratios (1:200 w/w) required (140, 152). More recently, a method that uses sucrose during liposome formation and protein reconstitution has provided a means for more rapid and improved reconstitution efficiency for MscS-like channels. Using the so-called "*sucrose method*," MscS can be reconstituted into soy azolectin liposomes as well as liposomes made of mixtures of pure lipids (*e.g.,* phosphatidylcholine, phosphatidylethanolamine, and phosphatidylglycerol) efficiently at a 1:1000 or a 1:4000 w/w ratio (12). This method—the first to demonstrate, *via* electrical recording, the co-reconstitution of MscS and MscL into liposomes—provides the added advantage of enabling fast and efficient reconstitution, with only 3 h of preparation

time required compared with typically 2 days for the traditional *Dehydration/Rehydration* (D/R) method. Both the D/R and sucrose methods have been widely used to study protein-lipid interactions in both pure and mixtures of lipids (104, 110, 123, 128, 129), revealing that the channel mechanosensitivity and clustering behavior are independently affected by their lipid environment (Fig. 5D).

Liposomes can also be prepared using an electroformation method, first described by Angelova and Dimitrov (3). Cell-sized vesicles and giant unilamellar liposomes have been successfully produced using this method (130). Only MscL of *E. coli* has been incorporated into liposomes using electro-formation, and functional characterization was demonstrated by Martinac and co-workers (37). An automated electro-formation method (Nanion Technologies GmbH, München, Germany) instead uses a solvent-free approach to produce the MscL-loaded giant liposomes (97).

Recording MscL and MscS activity in tethered bilayers

Recently tethered lipid bilayer technology has been used to study MscS and MscL function. This technology enables lipid bilayers to be attached to a lipid tether molecule, which is itself anchored to a gold electrode *via* a pyridyl disulphide or benzyl disulphide moiety (30). The technique creates a reservoir between the lipid membrane and the gold electrode. The gold electrode can then be referenced to another electrode to enable impedance spectroscopic measurements across the tethered bilayer (30) (Fig 6). When an alternating current potential is applied, ions will flow across the lipid membrane through ion channels to/from the external solution. How conductive the membrane becomes depends on the applied voltage and the state of any channel proteins residing in the tethered lipid membrane. Pulsed amperometry (in which transient voltages are applied to the system and the resulting transient current measured, from which the membrane conductance can be calculated) is employed to study voltage-dependent channel conductance in tethered lipid membranes. This allows novel measures of channel properties to be obtained. Tethered bilayer membranes permit application of very high voltages (up to 1 V; our unpublished data), whereas standard patch-clamp techniques become problematic for prolonged or high voltage because patch seals are readily broken at voltages significantly exceeding 100 mV. Petrov and co-workers (125) have observed a voltage-dependent conductance for membranes containing MscS but not in membranes containing MscL (Fig. 4C). Tethered bilayer membranes provide a robust, rapid screening platform for compounds that, for example, interfere with MscL and MscS gating, which could subsequently provide a molecular basis for developing novel types of antibacterial agents (see section on bacterial MS channels as potential drug targets).

Spectroscopic studies of MscL and MscS structural dynamics

EPR spectroscopy combined with patch-clamp recordings from both MscL and MscS channels has helped elucidate how the basic physical properties of the lipid bilayer, such as thickness, curvature, and/or pressure profile, affect conformational changes within the channel that accompany channel gating (32, 99, 120, 127).

For EPR spectroscopy, the introduction of a single cysteine residue into the MscL (123) or MscS protein (154) enables the channel to be labeled with a nitroxide spin label that is characterized by an N-O group containing the unpaired paramagnetic electron required to produce an EPR signal (101). The EPR signal can then be used to measure distances between the spin labels, enabling the spatial orientation of the secondary structural elements of MscL (121) and MscS (153) to be determined. Such experiments have enabled computational modeling of the channel structure to be undertaken with a spatial resolution at the level of the backbone fold (121, 153). In addition, micro-environment paramagnetic collisional probes have been used as relaxing agents to determine solvent accessibility and the polarity of the spin label. In experiments conducted by Perozo, Martinac, and co-workers (121–123), molecular oxygen as a relaxing agent enabled the location of the transmembrane channel domain to be determined, whereas the nickel-chelated complex Ni(II)-ethylene-diaminediacetate (NiEdda) was used as a relaxing agent to determine the location of the extracellular domains. Moreover, EPR has enabled the dynamic motion of the domains between the two environments to be visualized on a milli-second time scale.

FRET spectroscopy has mainly been used to study the open state of MscL. Similar to the EPR spectroscopic studies (121, 123), Corry *et al.* labeled specific MscL residues that had been mutated to cysteines with flurophores for FRET studies (31, 33). These studies enabled measurement of the open channel diameter for MscL at 69 Å, which correlated well with the open diameter of 70 Å measured by EPR (121). In contrast, however, the FRET studies indicate that the transition to the open state is less dramatic compared with previous open channel MscL models derived from EPR measurements. The improved open-state model suggests a much smaller conformational change from the closed to the open state (31), with the TM2 helix lying closer to the channel pore than in previously suggested models (18, 121, 141). Furthermore, the FRET studies found that the N-terminus remains anchored at the surface of the membrane, suggesting it can either guide the tilt of or directly translate membrane tension to the TM1 pore-lining helix.

In the case of MscS, Machiyama *et al.* (91) used FRET efficiency measurements to monitor liposome-reconstituted channel opening and closing in response to the addition of LPC. By fluorophore-labeling residues in the cytoplasmic domain of MscS, the authors of this study were able to demonstrate that the cytoplasmic portion of the protein undergoes a structural change when the channel opens.

FRET has also been used to demonstrate that certain lipid formulations promote the self-assembly of MscS protomers into two-dimensional clusters (152). The authors of this study discovered that inclusion of anionic lipids in their lipid mixture reduced the amount of clustering of MscS. More recently our group has used FRET in conjunction with fluorescence lifetime imaging to determine that MscL also self-assembles into clusters in lipid membranes and, furthermore, that MscS will also cluster with MscL (Fig. 7) (110).

Computational Modeling of MscL and MscS Structure and Function

A large number of MD simulations have been carried out since the publication of the first crystal structures of MscL and MscS (11, 24). These studies have largely focused on either
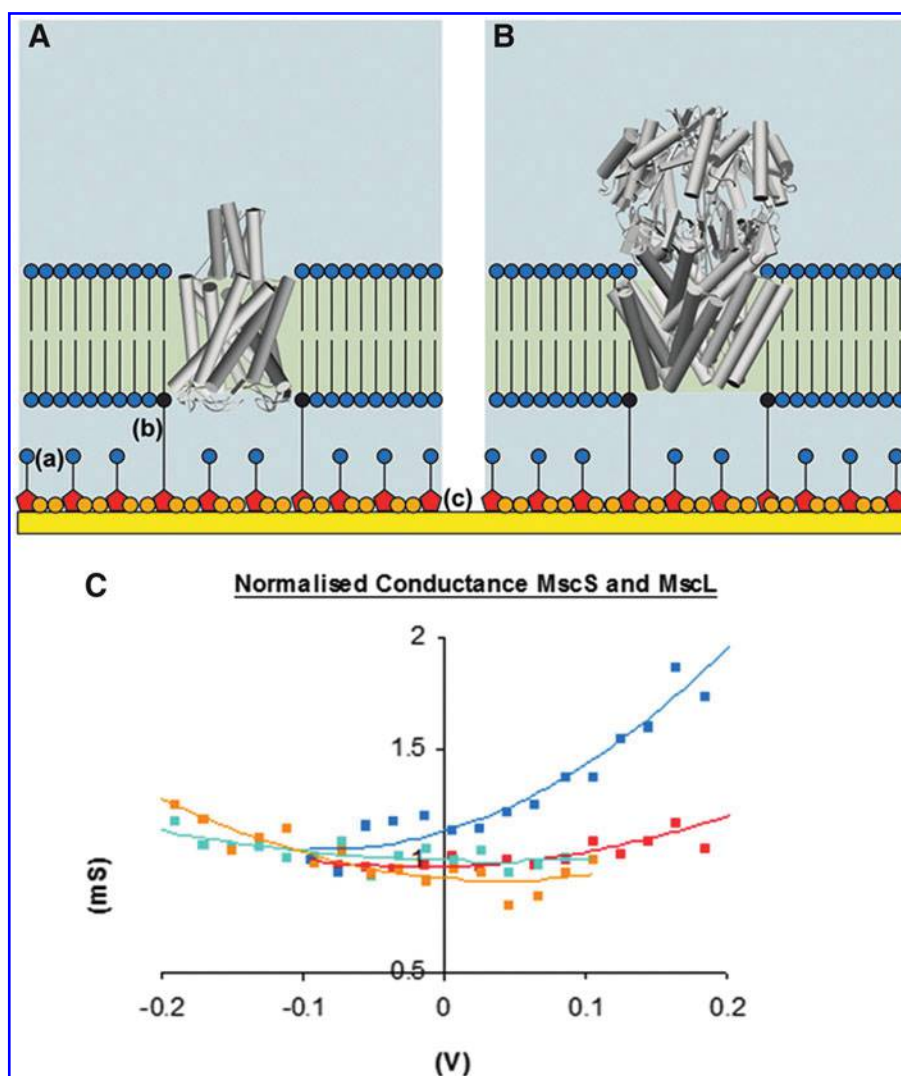
FIG. 6.   Electrical recording of MscL and MscS activity in tethered bilayers. Schematic of a tethered lipid bilayer containing **(A)** MscL and **(B)** MscS. Short hydrophilic spacer molecules (a) are interspersed with tethers (b) that anchor the lipid bilayer by penetrating the monolayer leaflet of the bilayer. The hydrophilic segment of the tether molecules is twice the length of the hydrophilic segment of the spacers. This is intended to permit accommodation of segments of the MscL or MscS that may protrude beyond the inner leaflet of the bilayer toward the tethering gold surface. Both the spacers and the lipid tethers are anchored to a gold electrode by sulfide chemistry (c). The region between the gold surface and the tethered lipid bilayer membrane forms an ionic reservoir permitting measurement of ion fluxes that pass through the membrane. The tethering sulfur groups also include a phenyl disulphide moiety that provides space between the tethers and spacers to facilitate ionic diffusion within the reservoir space. MscL and MscS can be reconstituted into the tethered bilayer, and impedance spectroscopy can then be used to measure the conductance across the membrane caused by the presence of the channels. **(C)** Normalized conductance–voltage relationship for MscS and MscL reconstituted into tethered bilayers. In C20 diphytanyl (70%) hydroxylglycerol (30%) tethered membranes: *MscS* conductance is voltage dependent and rectifying in the range $+100$ to -200 mV (*cyan squares*) and -100 to $+200$ mV (*blue squares*): *MscL* is essentially independent of voltage over the same range of $+100$ to -200 mV (*gold squares*) and -100 to $+200$ mV (*red squares*): Note that polarity is defined by the gold electrode tethering the membrane relative to the counter electrode. In the inner leaflet, 10% of the lipids were tethers and 90% were mobile. In the outer leaflet, all lipids were mobile. At the gold surface, the spacer groups are ~2 nm in length, and the thickness of the reservoir space between the gold and the inner surface of the membrane was ~4 nm in length. To see this illustration in color, the reader is referred to the web version of this article at www.liebertpub.com/ars

unraveling the structural changes or studying the lipid–protein interactions that occur during the closed to open state transitions on channel activation by membrane tension (32).

MD simulations of MscL have shown that without the use of biasing forces or large tension, partial or no opening of the pore is observed (29, 45, 53, 70). Different methods have been used to induce and accelerate the conformational changes,

including the application of radial forces (19, 52, 78) and different types of pressure and tension applied to the protein or the membrane (19, 29). As discussed in a review by Corry and Martinac (32), the structural changes observed in these studies depend on the nature and magnitude of the forces applied, and, in some cases, the order of events might not be reliable. Furthermore, the use of radial forces can bias the movement of
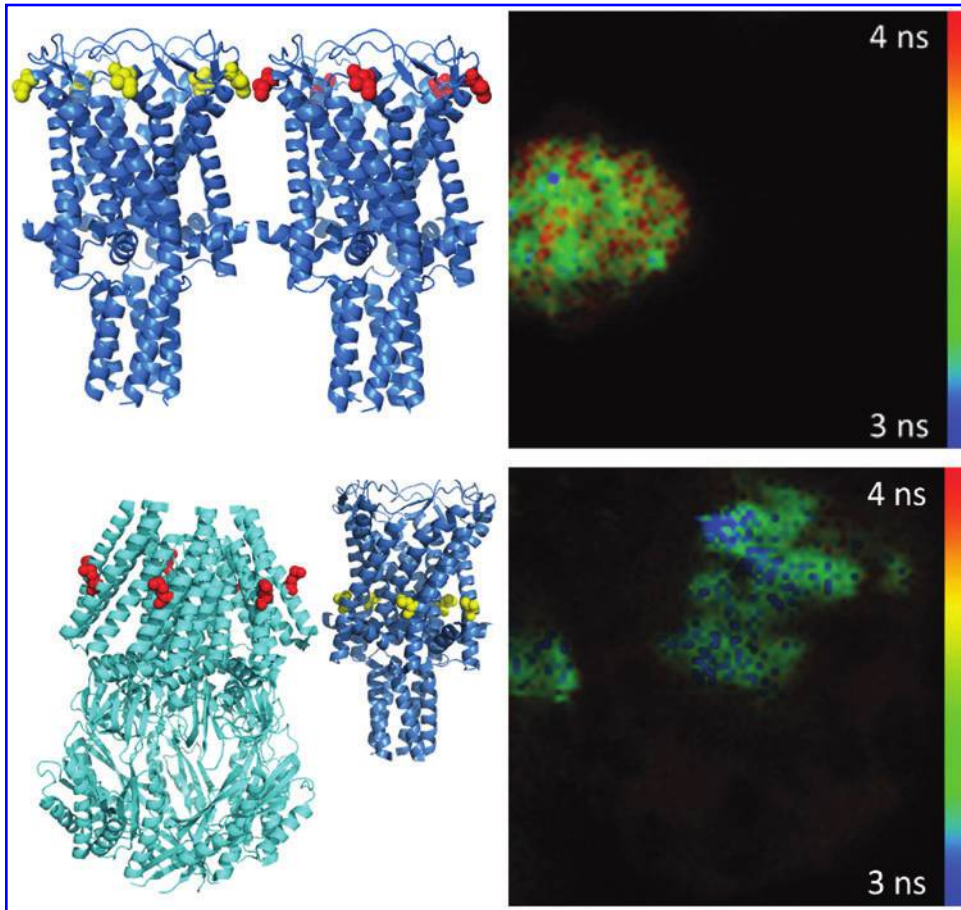
FIG. 7. Clustering of bacterial MS channels. Fluorescence Lifetime (FLIM)–Förster Resonance Energy Transfer (FRET) Images (FLIM-FRET images) showing clustering of MscL with other MscL molecules (*Top*), and MscL molecules with MscS molecules (*Bottom*) in lipids. The FRET between donor and acceptor fluorescence molecules of the separately labeled populations results in the fluorescence of the donor molecule having a reduced fluorescence lifetime (blue regions in the right-hand images). This reduced lifetime indicates regions in which the two fluorescently labeled populations are in very close proximity. Images taken from (110) with permission. To see this illustration in color, the reader is referred to the web version of this article at www.liebertpub.com/ars

the protein in a particular direction, and the use of large forces or tension can distort the protein. This can be avoided by simulating the protein in a curved lipid bilayer (103). Another alternative is to incorporate structural data from experiments into MD simulations, as in a recent study by Corry and colleagues in which experimentally derived distances from 80 FRET-derived distance constraints and 640 EPR constraints were used to model the open pore of MscL (31).

A major challenge of modeling membrane proteins such as MscL and MscS is that atomistic MD simulations are usually limited to a few hundred nanoseconds. A number of more recent studies have, therefore, used coarse-grained MD simulations to extend simulations into the microsecond range (40, 90, 164) and combined coarse-grained simulations with experimental restraints to model the open pore of MscL and investigate the structural changes induced by membrane thinning. In addition to the above MD simulations, the gating of MscL has also been investigated using different modeling techniques such as normal mode analysis (150) and finite element methods (145, 146).

All the aforementioned MD simulation studies focused on the gating mechanism of MS channels. Another series of simulations focuses on the interactions of MscL with the surrounding lipid bilayer in order to shed light on how the protein senses the tension that subsequently induces gating. MD simulations by Elmore and Dougherty (46) of MscL in the presence of different lipids suggest that specific lipid-protein interactions might explain the different gating tension of

MscL in membranes of various lipid compositions. In contrast, simulations by Gullingsrud *et al.* (54) and Jeon and Voth (70) suggest that macroscopic forces, such as changes in lateral pressure profiles, for the most part, govern the structure and gating mechanism of MscL. Furthermore, simulations of MscL in lipids of different chain lengths suggest that membrane thinning causes structural changes in the protein to avoid a hydrophobic mismatch between protein and the lipid bilayer (39, 46). Analytical approaches (156, 157), coarse-grained MD (118), and free energy simulations (131) confirmed the importance of hydrophobic matching, lateral pressure profiles, and mechanical forces in the bilayer on the mechanism and energy profile of MscL gating.

In contrast to MscL, the major goal of simulation studies focused on MscS has been to determine whether the crystal structure (11) represents an open, closed, or inactivated conformation, or perhaps even a nonfunctional state of the channel. MD simulations of the pore-forming region (8) and the full-length protein (134) with the backbone particles constrained to the 3D crystal structure solved by Bass *et al.* (11) showed no wetting of the hydrophobic area or partial dehydration of the pore. In contrast, simulations of the gain-of-function mutant L109S resulted in a stable hydration of the entire pore region (8). Sotomayor and Schulten (134) reported a collapsing of the pore when the backbone constraints are removed, but a widening of the hydrophobic area and the formation of a stable, hydrated pore when surface tension is applied. Collectively, these results suggest that the MscS crystal structure by Bass *et al.* (11) is more

likely to represent a nonconducting inactivated state of the channel [see also review by Corry and Martinac (32)]. Furthermore, the crystal structure does not appear to be stable in a simulated lipid bilayer, calling into question whether this structure actually represents an *in vivo* functional state of the channel. The situation is further complicated by the fact that the dehydration and widening of the pore region may be voltage dependent (137).

Another way to determine the likely conductive state of the crystal structure is to simulate the flow of water or ions through the pore. The electrostatic properties and the ion conduction of MscS were also investigated using a new mesoscopic approach (135) for simulations of passive ion transport over long simulation times along with atomistic simulations using biasing electrostatic potentials (136). Both types of simulations showed low conductance for the state of the crystal structure but conductance levels in agreement with experimental data for an open state of the channel. Anishkin *et al.* (8) used steered MD simulations to move Cl^- ions through the narrow part of the pore, and the large energy barriers suggest a conductance that is too low for the crystal structure to represent an open state of the channel.

Even if the crystal structure of MscS does not represent the closed or open state of the channel, the structure can still be useful as a starting point for simulations. Anishkin *et al.* (7) used a newly developed simulation method to model a more compact conformation that better approximates the closed state of the channel. This closed state is stable in a lipid bilayer and nonconducting over a range of physiological voltages. Vasquez *et al.* (154) modeled the closed state of MscS using MD simulations with restraints based on solvent accessibility data from EPR experiments. Both groups of authors used their closed state models to determine the structure of the fully open state channel. As seen in simulations of MscL, the use of biasing forces was required to induce the transition between closed and open states. Anishkin *et al.* (7) obtained an open pore structure from simulations that involve a sequence of extrapolation-minimization cycles followed by refinement of the structure using atomistic MD simulations. The conductance and in-plane expansion of the open pore model is in agreement with experimental data. Vasquez *et al.* (153) employed a combination of rigid body transformations followed by MD simulations that incorporated solvent accessibility data from EPR experiments and a bias to induce pore opening. Belyy *et al.* (14) used steered MD simulations to observe the transition between closed and open state for the wild type and the loss-of-function mutant F68S. The simulations of the wild type produced a hydrated pore, while simulations of the mutant showed a different hydration pattern and structure of the TM helices that is consistent with the mutants' tendency toward inactivation observed experimentally. Different simulation techniques at the atomistic and mesoscopic level (47, 135, 136) have also been employed to investigate the role of the cytoplasmic domain in the conductance of anions and cations through the channel.

The Role of Redox Signaling in Regulation of Bacterial MS Channels

Redox reactions are involved in all cellular processes. The ability to control such stresses resulting from redox reactions is pivotal to bacterial survival, and the reader is directed to ex-cellent reviews by Okegbe (116), Chen (25), Oktyabrskii (117), and Green [(51) and reviews therein] on the subject of bacterial redox sensors and metabolites. To the best of our knowledge, there are no known scientific reports on whether there is a direct link between bacterial redox signaling and regulation of MS channels in bacteria. However, a very recent and exciting discovery of the mechanosensitivity of the eukaryotic Piezo1 and Piezo2 cationic channels (34, 35) may give some insight into possible new mechanisms for cell volume regulation and redox signaling. For example, it was recently shown that mutations in Piezo1 may be implicated in hereditary Xerocytosis (168), a hemolytic anemia that is characterized by primary erythrocyte dehydration. The authors postulated that Piezo1 may serve as a cell swelling sensor. Mutations in the channel, resulting in gradual dehydration of the erythrocytes, are associated with changes in oxygenation/deoxygenation, where the deoxygenated, circulating erythrocytes exhibit reversible increases in cation permeability (49, 87). Regulation of oxygen and its associated redox reactions is essential in bacteria. Whether or not there may be interactions between the bacterial oxygenation level and cellular volume is presently unknown; however, the findings previously made in eukaryotic cells may have exciting implications for bacterial systems. For example, the family of MscS-like channels is highly diverse with this subfamily of channels existing not only in bacteria, but also archaea and plants (65, 96, 126). The structurally simplest prototype member of the family is MscS. However, many MscS homologues are structurally more complex and possess additional transmembrane helices (65). In addition, from the six MscS-like channels in *E. coli,* there seem to be additional regulatory requirements for them to function as MS channels (65). These may also include redox signaling. Interestingly, it has been reported that under hypo-osmotic shock, the redox potential in *E. coli* cells drops but is reversed by sulfhydryl reagents (117). Increasing the osmotic pressure in glucose-starved *E. coli* cells causes such cells to start to accumulate glutathione from the extra-cellular medium, which is accompanied by simultaneous K^+ and glutamate accumulation characteristic of the initial stage of *E. coli* response to osmotic shock (158). In this context, it is worth mentioning that MscCG of the soil bacterium *C. glutamicum* was shown to be a component of a pump/leak mechanism regulating glutamate transport under hyperosmotic conditions (21), which suggests that MscS-like channels may also be involved in redox signaling in bacteria. Indirect mechanisms may also exist through which redox signaling affects MS channel function. For example, a *Pseudomonas* bacterium produces redox-active phenazines in order to kill off competing fungi (147) through generation of reactive oxygen species (ROS). Production of zwitterionic pyocyanins by *Pseudomonas aeruginosa* also induces acute nosocomial pneumonia in humans through ROS generation (84, 112). Besides their redox activity, the zwitterionic nature of many of the phenazines and pyocyanins means that they could readily insert into the cell membrane and, therefore, may also act as amphipaths, possibly influencing MS channel gating.

Medical and Research Applications of Bacterial MS Channels

Bacterial MS channels as nanodevices

MscL produces a nonselective pore that is ~3 nm in diameter when activated (33, 38), and it has been shown that

protein complexes of approximately 6.5 kDa are able to pass through the open MscL pore unhindered (2, 17, 151). The channel activates in response to changes in membrane tension without the aid of other components and is highly stable, as shown in the conservation of its gating functionality after purification and reconstitution into lipid vesicles (58). Reconstitution of MscL can be carried out using a variety of different lipids (50), and the channel is readily engineered (77) with the inclusion of gain-and-loss-of-function mutants. These characteristics highlight the aptitude of MscL for use as a nanovalve in liposomal drug delivery systems.

The uses of liposomes as particulate drug delivery vehicles are mostly found in the administration of highly toxic compounds such as those used in cancer chemotherapy and fungal treatments (69, 106, 113). The encapsulation of these compounds within liposomes allows the drug to maintain its efficacy while minimizing its toxicity when compared with the drug's free form. Liposomes also provide a high degree of bio-compatibility and are capable of protecting encapsulated cargoes from degrading enzymes, thereby increasing the mean residence time of drugs within the body. Liposomes have also found use in vaccine delivery and as carriers for gene therapy (26, 148). In general, liposomes rely heavily on the use of specific lipid formulations to achieve a variety of effects that range from efficiency in drug encapsulation, triggers for release, site accumulation, and prolonged half-life *in vivo*. Of most interest to this discussion, however, is the use of light activated nanovalves, based on mutant MscL channels that activate when exposed to ultraviolet light. (77). By coupling a photosensitive compound into the 22nd amino acid position of MscL, Kocer and co-workers were able to demonstrate the reversible activation of MscL in liposome bilayers. More generally, this work demonstrates a biocompatible, reversible, method for introducing a charge into the MscL channel gate that activates the channel, and thus paves the way for further exciting studies in this area.

Bacterial MS channels as potential drug targets

Multidrug-resistance in pathogenic strains of bacteria is increasingly a problem in the treatment of bacterial infections and diseases. The re-emergence of tuberculosis is one of the serious threats that are spreading rapidly throughout the world. Furthermore, many strains of enterococci, *S. aureus*, and *Clostridium difficile* have acquired resistance to vancomycin, the last antibiotic that was still able to fight them successfully. Many new antibiotics merely represent modifications of existing compounds, exacerbating the need for novel approaches in designing new types of antibiotics.

Bacterial MS channels exhibit strong homology across all bacteria (Fig. 2), and disruption of their function causes slowing or impairment of bacterial growth. Previously, it was shown that parabens (a class of antimicrobial agents) and some amphipaths (a class of compounds with hydrophobic and hydrophilic properties) selectively interfere with bacterial MS channels and inhibit growth by opening the channels, thereby collapsing the cell turgor and causing leakage of cytoplasmic contents (71, 72, 94, 108). For example, using the Autodock program Nguyen *et al.* (108) calculated a binding energy of 4.91 kcal/mol (8.3 kT) for propyl paraben binding to the gate of MscL of *M. tuberculosis*. This binding energy cor-
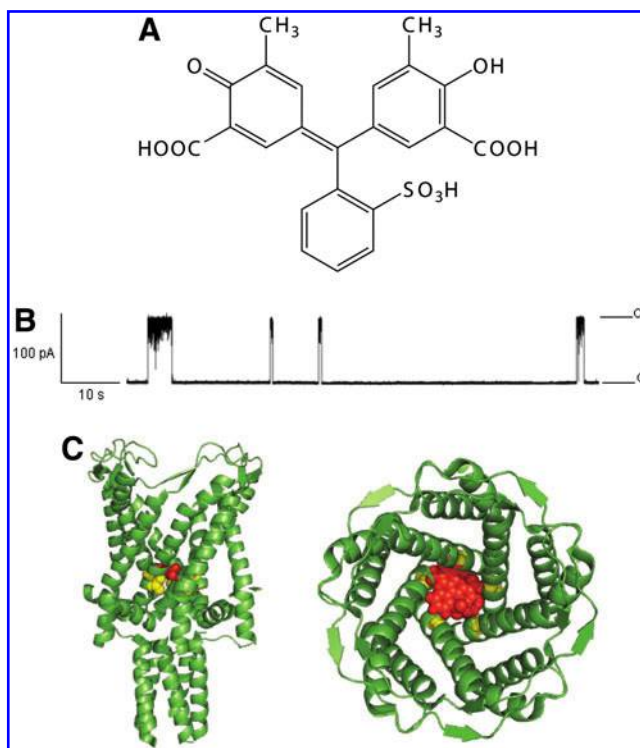

FIG. 8.　Activation of MscL by ECR. (A) Structure of the triphenylmethane dye ECR (160). **(B)** Current trace of spontaneous activity of MscL in the presence of 250 μM ECR. ECR was added to the bath solution. Pipette voltage was $+30$ mV. C and O1 denote a closed and open channel current level, respectively. **(C)** Predicted binding of ECR (red spheres) in the pore of the channel close to the cytoplasmic side of the *E. coli* MscL. ECR, Eriochrome cyanine R. To see this illustration in color, the reader is referred to the web version of this article at www.liebertpub.com/ars

responds to a concentration of ~ 0.25 mM of propyl paraben, which was shown in patch-clamp experiments to be sufficient to induce brief spontaneous activity of MscL. Furthermore, a screen of more than 2000 substances using the Autodock program helped identify eriochrome cyanine R as a compound that can bind to the hydrophobic lock of MscL with energy of 11.27 kcal/mol (~ 19 kT) (Fig. 8). This energy was shown to be sufficient to induce frequent and relatively long spontaneous openings of MscL in patch-clamp experiments (22, 107) (Martinac *et al.*, unpublished data). Consequently, compounds that interfere with MS channel function may, therefore, present novel agents for inhibiting growth of bacterial pathogens. Given that nonbacterial cells also contain MS channels, it will be important to identify agents which specifically interfere with the bacterial MscS and MscL channels but have no effect on MS channels in other organisms or human cells. This may be a lesser problem than one would expect, because no MscL- or MscS-like gene has been found within the human or any animal genome.

Research applications of bacterial MS channels

Most recently, MscL and MscS have found a new application in research on mammalian cells as conduits for rapid and controlled uptake of membrane-impermeable molecules (41).

G22C MscL mutants, which phenotypically exhibit charged cysteine residues in the pore of the protein, were functionally expressed in CHO and HEK-293 cells. They could then be forced into opening by the application of select methanethiosulfonate reagents (161, 165). MscL is well suited for this type of research because of its very large pore diameter and lack of ion selectivity (38), enabling molecules such as the fluorescent Alexa-Fluor molecules (~ 700 Da) and fluorescently labeled phalloidin (~ 1.3 kDa) to be delivered into live mammalian cells (41). Being able to transfect mammalian cells with this MscL mutant will open up exciting new possibilities for live-cell fluorescent staining and for the controlled intracellular delivery of various ligands.

Conclusions

MscL and MscS are, to date, the best studied types of MS channels, and much has been learned about the basic physical principles of mechanosensory transduction from the studies of their structure, function, and MD. Nevertheless, the molecular details of MscL and MscS interactions with the lipid bilayer still remain to be elucidated, in order to fully understand the mechanosensitivity of these fascinating membrane proteins. Ultimately, the acquired knowledge should lead to a better understanding of the basic molecular principles underlying mechanosensory transduction in living cells of different evolutionary provenances. From a practical viewpoint, the acquired knowledge could also be used to design MscL and/or MscS nanovalves for biomedical and engineering applications. Hence, the journey for scientists working on bacterial MS channels will continue and promises to be as exciting as the one of the last two decades.

Acknowledgments

References

1. Ajouz B, Berrier C, Besnard M, Martinac B, and Ghazi A. Contributions of the different extramembranous domains of the mechanosensitive ion channel MscL to its response to membrane tension. *J Biol Chem* 275: 1015–1022, 2000.
2. Ajouz B, Berrier C, Garrigues A, Besnard M, and Ghazi A. Release of thioredoxin via the mechanosensitive channel MscL during osmotic downshock of *Escherichia coli* cells. *J Biol Chem* 273: 26670–26674, 1998.
3. Angelova M and Dimitrov D. Liposome electroformation. *Faraday Discuss Chem Soc* 81: 303–311, 1986.
4. Anishkin A, Akitake B, and Sukharev S. Characterization of the resting MscS: modeling and analysis of the closed bacterial mechanosensitive channel of small conductance. *Biophys J* 94: 1252–1266, 2008.
5. Anishkin A, Chiang CS, and Sukharev S. Gain-of-function mutations reveal expanded intermediate states and a sequential action of two gates in MscL. *J Gen Physiol* 125: 155–170, 2005.
6. Anishkin A, Gendel V, Sharifi NA, Chiang CS, Shirinian L, Guy HR, and Sukharev S. On the conformation of the COOH-terminal domain of the large mechanosensitive channel MscL. *J Gen Physiol* 121: 227–244, 2003.
7. Anishkin A, Kamaraju K, and Sukharev S. Mechanosensitive channel MscS in the open state: modeling of the transition, explicit simulations, and experimental measurements of conductance. *J Gen Physiol* 132: 67–83, 2008.
8. Anishkin A and Sukharev S. Water dynamics and dewetting transitions in the small mechanosensitive channel MscS. *Biophys J* 86: 2883–2895, 2004.
9. Bae C, Gnanasambandam R, Nicolai C, Sachs F, and Gottlieb PA. Xerocytosis is caused by mutations that alter the kinetics of the mechanosensitive channel PIEZO1. *Proc Natl Acad Sci U S A* 110: E1162–E1168, 2013.
10. Balleza D and Gomez-Lagunas F. Conserved motifs in mechanosensitive channels MscL and MscS. *Eur Biophys J* 38: 1013–1027, 2009.
11. Bass RB, Strop P, Barclay M, and Rees D. Crystal structure of *Escherichia coli* MscS, a voltage-modulated and mechanosensitive channel. *Science* 298: 1582–1587, 2002.
12. Battle AR, Petrov E, Pal P, and Martinac B. Rapid and improved reconstitution of bacterial mechanosensitive ion channel proteins MscS and MscL into liposomes using a modified sucrose method. *FEBS Lett* 583: 407–412, 2009.
13. Bechstedt S and Howard J. Models of hair cell mechanotransduction. In: *Mechanosensitive Ion Channels, Part B*, edited by Hamill OP. San Diego: Academic Press, 2007, pp. 399–424.
14. Belyy V, Anishkin A, Kamaraju K, Liu N, and Sukharev S. The tension-transmitting 'clutch' in the mechanosensitive channel MscS. *Nat Struct Mol Biol* 17: 451–458, 2010.
15. Belyy V, Kamaraju K, Akitake B, Anishkin A, and Sukharev, S. Adaptive behavior of bacterial mechanosensitive channels is coupled to membrane mechanics. *J Gen Physiol* 135: 641–652, 2010.
16. Berrier C, Besnard M, Ajouz B, Coulombe A, and Ghazi A. Multiple mechanosensitive ion channels from *Escherichia coli*, activated at different thresholds of applied pressure. *J Membr Biol* 151: 175–187, 1996.
17. Berrier C, Garrigues A, Richarme G, and Ghazi A. Elongation factor Tu and DnaK are transferred from the cytoplasm to the periplasm of *Escherichia coli* during osmotic downshock presumably via the mechanosensitive channel mscL. *J Bacteriol* 182: 248–251, 2000.
18. Betanzos M, Chiang CS, Guy HR, and Sukharev S. A large iris-like expansion of a mechanosensitive channel protein induced by membrane tension. *Nat Struct Biol* 9: 704–710, 2002.
19. Bilston LE and Mylvaganam K. Molecular simulations of the large conductance mechanosensitive (MscL) channel under mechanical loading. *FEBS Lett* 512: 185–190, 2002.
20. Blount P, Sukharev SI, Moe PC, Schroeder MJ, Guy HR, and Kung C. Membrane topology and multimeric structure of a mechanosensitive channel protein of *Escherichia coli*. *EMBO J* 15: 4798–4805, 1996.
21. Börngen K, Battle AR, Moker N, Morbach S, Marin K, Martinac B, and Kramer R. The properties and contribution of the Corynebacterium glutamicum MscS variant to fine-tuning of osmotic adaptation. *Biochim Biophys Acta* 1798: 2141–2149, 2010.
22. Boulos RA. Antimicrobial dyes and mechanosensitive channels. *Antonie Van Leeuwenhoek* 104: 155–167, 2013.
23. Chalfie M. Neurosensory mechanotransduction. *Nat Rev Mol Cell Biol* 10: 44–52, 2009.
24. Chang G, Spencer RH, Lee AT, Barclay MT, and Rees DC. Structure of the MscL homolog from Mycobacterium

tuberculosis: a gated mechanosensitive ion channel. *Science* 282: 2220–2226, 1998.

25. Chen PR, Brugarolas P, and He CA. Redox signaling in human pathogens. *Antioxid Redox Signal* 14: 1107–1118, 2011.

26. Chen WC and Huang L. Non-viral vector as vaccine carrier. *Adv Genet* 54: 315–337, 2005.

27. Chetwynd AP, Scott KA, Mokrab Y, and Sansom MSP. CGDB: a database of membrane protein/lipid interactions by coarse-grained molecular dynamics simulations. *Mol Membr Biol* 25: 662–669, 2008.

28. Chiang CS, Anishkin A, and Sukharev S. Gating of the large mechanosensitive channel *in situ*: estimation of the spatial scale of the transition from channel population responses. *Biophys J* 86: 2846–2861, 2004.

29. Colombo G, Marrink SJ, and Mark AE. Simulation of MscL gating in a bilayer under stress. *Biophys J* 84: 2331–2337, 2003.

30. Cornell BA, Braach-Maksvytis VL, King LG, Osman PD, Raguse B, Wieczorek L, and Pace RJ. A biosensor that uses ion-channel switches. *Nature* 387: 580–583, 1997.

31. Corry B, Hurst AC, Pal P, Nomura T, Rigby P, and Martinac, B. An improved open-channel structure of MscL determined from FRET confocal microscopy and simulation. *J Gen Physiol* 136: 483–494, 2010.

32. Corry B and Martinac B. Bacterial mechanosensitive channels: experiment and theory. *Biochim Biophys Acta-Biomembr* 1778: 1859–1870, 2008.

33. Corry B, Rigby P, Liu ZW, and Martinac B. Conformational changes involved in MscL channel gating measured using FRET spectroscopy. *Biophys J* 89: L49–L51, 2005.

34. Coste B, Mathur J, Schmidt M, Earley TJ, Ranade S, Petrus MJ, Dubin AE, and Patapoutian A. Piezo1 and Piezo2 are essential components of distinct mechanically activated cation channels. *Science* 330: 55–60, 2010.

35. Coste B, Xiao B, Santos JS, Syeda R, Grandl J, Spencer KS, Kim SE, Schmidt M, Mathur J, Dubin AE, Montal M, and Patapoutian A. Piezo proteins are pore-forming subunits of mechanically activated channels. *Nature* 483: 176–181, 2012.

36. Cox CD, Nomura T, Ziegler CS, Campbell AK, Wann KT and Martinac B. Selectivity mechanism of the mechanosensitive channel MscS revealed by probing channel subconducting states. *Nat Commun* 4: 2137, 2013. doi: 10.1038/ncomms3137.

37. Cranfield CG, Kloda A, Petrov E, Battle A, Nomura T, Rohde P, Cox C, and Martinac B. Mechanosensitivity of Ion Channels. In: *Encyclopedia of Biophysics*, edited by Roberts GCK. Berlin, Heidelberg: Springer Verlag, 2012, pp. 1433–1440.

38. Cruickshank CC, Minchin RF, Le Dain AC, and Martinac B. Estimation of the pore size of the large-conductance mechanosensitive ion channel of *Escherichia coli*. *Biophys J* 73: 1925–1931, 1997.

39. Debret G, Valadie H, Stadler AM, and Etchebest C. New insights of membrane environment effects on MscL channel mechanics from theoretical approaches. *Proteins* 71: 1183–1196, 2008.

40. Deplazes E and Corry B. Structural investigation of MscL gating using experimental data and coarse grained MD simulations. *PLoS Comput Biol* 8: e1002683, 2012.

41. Doerner JF, Febvay S, and Clapham DE. Controlled delivery of bioactive molecules into live cells using the bacterial mechanosensitive channel MscL. *Nat Commun* 3: 990, 2012.

42. Dorwart MR, Wray R, Brautigam CA, Jiang Y, and Blount P. S. aureus MscL is a pentamer *in vivo* but of variable stoi-

chiometries *in vitro*: implications for detergent-solubilized membrane proteins. *PLoS Biol* 8: e1000555, 2010.

43. Edwards MD, Bartlett W, and Booth IR. Pore mutations of the *Escherichia coli* MscS channel affect desensitization but not ionic preference. *Biophys J* 94: 3003–3013, 2008.

44. Edwards MD, Black S, Rasmussen T, Rasmussen A, Stokes NR, Stephen T-L, Miller S, and Booth IR. Characterization of three novel mechanosensitive channel activities in *Escherichia coli*. *Channels* 6: 272–281, 2012.

45. Elmore DE and Dougherty DA. Molecular dynamics simulations of wild-type and mutant forms of the Mycobacterium tuberculosis MscL channel. *Biophys J* 81: 1345–1359, 2001.

46. Elmore DE and Dougherty DA. Investigating lipid composition effects on the mechanosensitive channel of large conductance (MscL) using molecular dynamics simulations. *Biophys J* 85: 1512–1524, 2003.

47. Gamini R, Sotomayor M, Chipot C, and Schulten K. Cytoplasmic domain filter function in the mechanosensitive channel of small conductance. *Biophys J* 101: 80–89, 2011.

48. Gillespie PG and Walker RG. Molecular basis of mechanosensory transduction. *Nature* 413: 194–202, 2001.

49. Gottlieb PA and Sachs F. Piezo1: properties of a cation selective mechanical channel. *Channels (Austin)* 6: 214–219, 2012.

50. Grage SL, Keleshian AM, Turdzeladze T, Battle AR, Tay WC, May RP, Holt SA, Contera SA, Haertlein M, Moulin M, Pal P, Rohde PR, Forsyth VT, Watts A, Huang KC, Ulrich AS, and Martinac B. Bilayer-mediated clustering and functional interaction of MscL channels. *Biophys J* 100: 1252–1260, 2011.

51. Green J and Paget MS. Bacterial redox sensors. *Nat Rev Microbiol* 2: 954–966, 2004.

52. Gullingsrud J and Schulten K. Gating of MscL studied by steered molecular dynamics. *Biophys J* 85: 2087–2099, 2003.

53. Gullingsrud J, Kosztin D, and Schulten K. Structural determinants of MscL gating studied by molecular dynamics simulations. *Biophys J* 80: 2074–2081, 2001.

54. Gullingsrud J and Schulten K. Lipid bilayer pressure profiles and mechanosensitive channel gating. *Biophys J* 86: 3496–3509, 2004.

55. Hamill OP and Martinac B. Molecular basis of mechanotransduction in living cells. *Physiol Rev* 81: 685–740, 2001.

56. Hamill OP, Marty A, Neher E, Sakmann B, and Sigworth FJ. Improved patch-clamp techniques for high-resolution current recording from cells and cell-free membrane patches. *Pflugers Arch* 391: 85–100, 1981.

57. Häse CC, Le Dain AC, and Martinac B. Molecular dissection of the large mechanosensitive ion channel (MscL) of *E. coli*: mutants with altered channel gating and pressure sensitivity. *J Membr Biol* 157: 17–25, 1997.

58. Häse CC, Le Dain AC, and Martinac B. Purification and functional reconstitution of the recombinant large mechanosensitive ion channel (MscL) of *Escherichia coli*. *J Biol Chem* 270: 18329–18334, 1995.

59. Häse CC, Minchin RF, Kloda A, and Martinac B. Cross-linking studies and membrane localization and assembly of radiolabelled large mechanosensitive ion channel (MscL) of *Escherichia coli*. *Biochem Biophys Res Commun* 232: 777–782, 1997.

60. Haswell ES. MscS-like proteins in plants. In: *Mechanosensitive Ion Channels Part A*, edited by Hamill OP. Amsterdam: Academic Press, 2007, pp. 329–359.

61. Haswell ES, Phillips R, and Rees DC. Mechanosensitive channels: what can they do and how do they do it? *Structure* 19: 1356–1369, 2011.

62. Hodgkin AL. 1963. The Ionic Basis of Nervous Conduction. http://nobelprize.org/medicine/laureates/1963/hodgkin-lecture.html (Accessed August 2, 2013).

63. Hodgkin AL and Huxley AF. Propagation of electrical signals along giant nerve fibers. *Proc R Soc Lond B Biol Sci* 140: 177–183, 1952.

64. Hodgkin AL and Huxley AF. A quantitative description of membrane current and its application to conduction and excitation in nerve. *J Physiol* 117: 500–544, 1952.

65. Howard J and Hudspeth AJ. Compliance of the hair bundle associated with gating of mechanoelectrical transduction channels in the bullfrog's saccular hair cell. *Neuron* 1: 189–199, 1988.

66. Huxley AF. 1963. The Quantitative Analysis of Excitation and Conduction in Nerve. http://nobelprize.org/nobel_prizes/medicine/laureates/1963/huxley-lecture.html (Accessed August 2, 2013).

67. Iscla I and Blount P. Sensing and responding to membrane tension: the bacterial MscL channel as a model system. *Biophys J* 103: 169–174, 2012.

68. Iscla I, Wray R, and Blount P. On the structure of the N-terminal domain of the MscL channel: helical bundle or membrane interface. *Biophys J* 95: 2283–2291, 2008.

69. Janoff AS. *Liposomes: Rational Design*. New York, NY: Marcel Dekker, 1999.

70. Jeon J and Voth GA. Gating of the mechanosensitive channel protein MscL: the interplay of membrane and protein. *Biophys J* 94: 3497–3511, 2008.

71. Kamaraju K, Akitake B, and Sukharev S. Membrane-perturbing capacity of parabens and their effects on a mechanosensitive channel directly correlate with hydrophobicity. *Biophys J* 94 (Supplement): 204, 2008.

72. Kamaraju K and Sukharev S. The membrane lateral pressure-perturbing capacity of parabens and their effects on the mechanosensitive channel directly correlate with hydrophobicity. *Biochemistry* 47: 10540–10550, 2008.

73. Kloda A, Ghazi A, and Martinac B. C-terminal charged cluster of MscL, RKKEE, functions as a pH sensor. *Biophys J* 90: 1992–1998, 2006.

74. Kloda A and Martinac B. Molecular identification of a mechanosensitive channel in archaea. *Biophys J* 80: 229–240, 2001.

75. Kloda A and Martinac B. Structural and functional differences between two homologous mechanosensitive channels of Methanococcus jannaschii. *EMBO J* 20: 1888–1896, 2001.

76. Kloda A and Martinac B. Mechanosensitive channels of bacteria and archaea share a common ancestral origin. *Eur Biophys J* 31: 14–25, 2002.

77. Kocer A, Walko M, and Feringa BL. Synthesis and utilization of reversible and irreversible light-activated nano-valves derived from the channel protein MscL. *Nat Protoc* 2: 1426–1437, 2007.

78. Kong YF, Shen YF, Warth TE, and Ma JP. Conformational pathways in the gating of *Escherichia coli* mechanosensitive channel. *Proc Natl Acad Sci U S A* 99: 5999–6004, 2002.

79. Kubalski A and Martinac B (Ed). *Bacterial Ion Channels and Their Eukaryotic Homologues*. Washington, DC: ASM Press, 2005.

80. Kumánovics A, Levin G, and Blount P. Family ties of gated pores: evolution of the sensor module. *FASEB J* 16: 1623–1629, 2003.

81. Kung C. A possible unifying principle for mechanosensation. *Nature* 436: 647–654, 2005.

82. Kung C, Martinac B, and Sukharev S. Mechanosensitive channels in microbes. *Annu Rev Microbiol* 64: 313–329, 2010.

83. Kung C, Saimi Y, and Martinac, B. Mechanosensitive ion channels in microbes and the early evolutionary origin of solvent sensing. In: *Current Topics in Membranes and Transport*, edited by Claudio T. New York: Academic Press, 1990, pp. 9451–9455.

84. Lau GW, Hassett DJ, Ran H, and Kong F. The role of pyocyanin in Pseudomonas aeruginosa infection. *Trends Mol Med* 10: 599–606, 2004.

85. Le Dain AC, Saint N, Kloda A, Ghazi A, and Martinac B. Mechanosensitive ion channels of the archaeon Haloferax volcanii. *J Biol Chem* 273: 12116–12119, 1998.

86. Levina N, Totemeyer S, Stokes NR, Louis P, Jones MA, and Booth IR. Protection of *Escherichia coli* cells against extreme turgor by activation of MscS and MscL mechanosensitive channels: identification of genes required for MscS activity. *EMBO J* 18: 1730–1737, 1999.

87. Lew VL and Bookchin RM. Ion transport pathology in the mechanism of sickle cell dehydration. *Physiol Rev* 85: 179–200, 2005.

88. Li Y, Wray R, Eaton C, and Blount P. An open-pore structure of the mechanosensitive channel MscL derived by determining transmembrane domain interactions upon gating. *FASEB J* 23: 2197–2204, 2009.

89. Liu Z, Gandhi CS, and Rees DC. Structure of a tetrameric MscL in an expanded intermediate state. *Nature* 461: 120–124, 2009.

90. Louhivuori M, Risselada HJ, van der Giessen E, and Marrink SJ. Release of content through mechano-sensitive gates in pressurized liposomes. *Proc Natl Acad Sci U S A* 107: 19856–19860, 2010.

91. Machiyama H, Tatsumi H, and Sokabe M. Structural changes in the cytoplasmic domain of the mechanosensitive channel MscS during opening. *Biophys J* 97: 1048–1057, 2009.

92. Maksaev G, Milac A, Anishkin A, Guy HR, and Sukharev S. Analyses of gating thermodynamics and effects of deletions in the mechanosensitive channel TREK-1: comparisons with structural models. *Channels (Austin)* 5: 34–42, 2011.

93. Martinac B. Bacterial mechanosensitive channels as a paradigm for mechanosensory transduction. *Cell Physiol Biochem* 28: 1051–1060, 2011.

94. Martinac B, Adler J, and Kung C. Mechanosensitive ion channels of *E. coli* activated by amphipaths. *Nature* 348: 261–263, 1990.

95. Martinac B, Buechner M, Delcour AH, Adler J, and Kung C. Pressure-sensitive ion channel in *Escherichia coli*. *Proc Natl Acad Sci U S A* 84: 2297–2301, 1987.

96. Martinac B and Kloda A. Evolutionary origins of mechanosensitive ion channels. *Prog Biophys Mol Biol* 82: 11–24, 2003.

97. Martinac B, Rohde PR, Battle AR, Petrov E, Pal P, Foo AF, Vasquez V, Huynh T, and Kloda A. Studying mechanosensitive ion channels using liposomes. *Methods Mol Biol* 606: 31–53, 2010.

98. Martinac B, Rohde PR, Cranfield CG, and Nomura T. Patch clamp electrophysiology for the study of bacterial ion channels in giant spheroplasts of *E. coli*. In: *Bacterial Cell Surfaces: Methods and Protocols*, edited by Delcour AH. New York: Springer Verlag, 2013, pp. 367–380.

99. Martinac B, Saimi Y, and Kung C. Ion channels in microbes. *Physiol Rev* 88: 1449–1490, 2008.

100. Maurer JA and Dougherty DA. Generation and evaluation of a large mutational library from the *Escherichia coli* mechanosensitive channel of large conductance, MscL: implications for channel gating and evolutionary design. *J Biol Chem* 278: 21076–21082, 2003.

101. Mchaourab H and Perozo E. Determination of protein folds and conformational dynamics using spin-labeling EPR Spectroscopy. In: *In Biological Magnetic Resonance*, edited by Eaton GES and Berliner L. New York: Kluwer-Plenum, 2000, pp. 155–218.

102. Meyer GR. *Electron Paramagentic Spectroscopy and Computer Modelling Studies of the Structure of Prokaryotic Mehanosensitive Channels*. Brisbane: University of Queensland, 2007, p. 132.

103. Meyer GR, Gullingsrud J, Schulten K, and Martinac B. Molecular dynamics study of MscL interactions with a curved lipid bilayer. *Biophys J* 91: 1630–1637, 2006.

104. Moe P and Blount P. Assessment of potential stimuli for mechano-dependent gating of MscL: effects of pressure, tension, and lipid headgroups. *Biochemistry* 44: 12239–12244, 2005.

105. Nakayama Y, Fujiu K, Sokabe M, and Yoshimura K. Molecular and electrophysiological characterization of a mechanosensitive channel expressed in the chloroplasts of Chlamydomonas. *Proc Natl Acad Sci U S A* 104: 5883–5888, 2007.

106. Ng AW, Wasan KM, and Lopez-Berestein G. Development of liposomal polyene antibiotics: an historical perspective. *J Pharm Pharm Sci* 6: 67–83, 2003.

107. Nguyen T. *The Pharmacology of the Mechanosensitive Channels of* Escherichia coli. Perth, Western Australia: The University of Western Australia, 2007, p. 137.

108. Nguyen T, Clare B, Guo W, and Martinac B. The effects of parabens on the mechanosensitive channels of *E. coli. Eur Biophys J* 34: 389–395, 2005.

109. Nomura T, Battle AR, and Martinac B. Lipid and lyso-lipid effects on the mechanosensitivity of liposome co-reconstituted MscS and MscL. *Biophys J* 100: 1514, 2011.

110. Nomura T, Cranfield CG, Deplazes E, Owen DM, Macmillan A, Battle AR, Constantine M, Sokabe M, and Martinac B. Differential effects of lipids and lyso-lipids on the mechanosensitivity of the mechanosensitive channels MscL and MscS. *Proc Natl Acad Sci U S A* 109: 8770–8775, 2012.

111. Nomura T, Sokabe M, and Yoshimura K. Lipid-protein interaction of the MscS mechanosensitive channel examined by scanning mutagenesis. *Biophys J* 91: 2874–2881, 2006.

112. O'Malley YQ, Reszka KJ, Rasmussen GT, Abdalla MY, Denning GM, and Britigan BE. The Pseudomonas secretory product pyocyanin inhibits catalase activity in human lung epithelial cells. *Am J Physiol Lung Cell Mol Physiol* 285: L1077–L1086, 2003.

113. O'Shaughnessy J. Liposomal anthracyclines for breast cancer: overview. *Oncologist* 8 Suppl 2: 1–2, 2003.

114. Oakley AJ, Martinac B, and Wilce MC. Structure and function of the bacterial mechanosensitive channel of large conductance. *Protein Sci* 8: 1915–1921, 1999.

115. Okada K, Moe PC, and Blount P. Functional design of bacterial mechanosensitive channels. Comparisons and contrasts illuminated by random mutagenesis. *J Biol Chem* 277: 27682–27688, 2002.

116. Okegbe C, Sakhtah H, Sekedat MD, Price-Whelan A, and Dietrich LE. Redox eustress: roles for redox-active metabolites in bacterial signaling and behavior. *Antioxid Redox Signal* 16: 658–667, 2012.

117. Oktyabrskii ON and Smirnova GV. Redox potential changes in bacterial cultures under stress conditions. *Microbiology* 81: 131–142, 2012.

118. Ollila OH, Risselada HJ, Louhivuori M, Lindahl E, Vattulainen I, and Marrink SJ. 3D pressure field in lipid membranes and membrane-protein complexes. *Phys Rev Lett* 102: 078101, 2009.

119. Ou X, Blount P, Hoffman RJ, and Kung C. One face of a transmembrane helix is crucial in mechanosensitive channel gating. *Proc Natl Acad Sci U S A* 95: 11471–11475, 1998.

120. Perozo E. Gating prokaryotic mechanosensitive channels. *Nat Rev Mol Cell Biol* 7: 109–119, 2006.

121. Perozo E, Cortes DM, Sompornpisut P, Kloda A, and Martinac B. Open channel structure of MscL and the gating mechanism of mechanosensitive channels. *Nature* 418: 942–948, 2002.

122. Perozo E, Kloda A, Cortes DM, and Martinac B. Sitedirected spin-labeling analysis of reconstituted Mscl in the closed state. *J Gen Physiol* 118: 193–206, 2001.

123. Perozo E, Kloda A, Cortes DM, and Martinac B. Physical principles underlying the transduction of bilayer deformation forces during mechanosensitive channel gating. *Nat Struct Biol* 9: 696–703, 2002.

124. Petrov E, Palanivelu D, Constantine M, Rohde PR, Cox CD, Nomura T, Minor DL, Jr., and Martinac B. Patch-clamp characterization of the MscS-like mechanosensitive channel from *Silicibacter pomeroyi. Biophys J* 104: 1426–1434, 2013.

125. Petrov E, Rohde PR, Cornell B, and Martinac B. The protective effect of osmoprotectant TMAO on bacterial mechanosensitive channels of small conductance MscS/MscK under high hydrostatic pressure. *Channels* 6: 262–271, 2012.

126. Pivetti CD, Yen MR, Miller S, Busch W, Tseng YH, Booth IR, and Saier MH, Jr. Two families of mechanosensitive channel proteins. *Microbiol Mol Biol Rev* 67: 66–85, table of contents, 2003.

127. Pliotas C, Ward R, Branigan E, Rasmussen A, Hagelueken G, Huang H, Black SS, Booth IR, Schiemann O, and Naismith JH. Conformational state of the MscS mechanosensitive channel in solution revealed by pulsed electronelectron double resonance (PELDOR) spectroscopy. *Proc Natl Acad Sci U S A* 109: E2675–E2682, 2012.

128. Powl AM, East JM, and Lee AG. Different effects of lipid chain length on the two sides of a membrane and the lipid annulus of MscL. *Biophys J* 93: 113–122, 2007.

129. Powl AM, East JM, and Lee AG. Anionic phospholipids affect the rate and extent of flux through the mechanosensitive channel of large conductance MscL. *Biochemistry* 47: 4317–4328, 2008.

130. Puff N and Angelova MI. Lipid vesicles-development and applications for studding membrane Heterogeneity and Interactions. *Adv Planar Lipid Bilayers Liposomes* 5: 173–228, 2006.

131. Rui H, Kumar R, and Im W. Membrane tension, lipid adaptation, conformational changes, and energetics in MscL gating. *Biophys J* 101: 671–679, 2011.

132. Ruthe HJ and Adler J. Fusion of bacterial spheroplasts by electric fields. *Biochim Biophys Acta* 819: 105–113, 1985.

133. Sachs F. Stretch-activated ion channels: what are they? *Physiology (Bethesda)* 25: 50–56, 2010.

134. Sotomayor M and Schulten K. Molecular dynamics study of gating in the mechanosensitive channel of small conductance MscS. *Biophys J* 87: 3050–3065, 2004.

135. Sotomayor M, van der Straaten TA, Ravaioli U, and Schulten K. Electrostatic properties of the mechanosensitive channel of small conductance MscS. *Biophys J* 90: 3496–3510, 2006.

136. Sotomayor M, Vasquez V, Perozo E, and Schulten K. Ion conduction through MscS as determined by electrophysiology and simulation. *Biophys J* 92: 886–902, 2007.

137. Spronk SA, Elmore DE, and Dougherty DA. Voltage-dependent hydration and conduction properties of the hydrophobic pore of the mechanosensitive channel of small conductance. *Biophys J* 90: 3555–3569, 2006.

138. Steinbacher S, Bass R, Strop P, and Rees DC. Structures of the prokaryotic mechanosensitive channels MscL and MscS. In: *Mechanosensitive Ion Channels, Part A*, San Diego: Elsevier Academic Press, Inc., 2007, pp. 1–24.

139. Steinbacher S, Bass R, Strop P, and Rees DC. 2007. Mechanosensitive Channel of Large Conductance (MscL) PDB. http://www.pdb.org/pdb/explore/explore.do? structure Id = 2OAR (Accessed date August 2, 2013).

140. Sukharev S. Purification of the small mechanosensitive channel of *Escherichia coli* (MscS): the subunit structure, conduction, and gating characteristics in liposomes. *Biophys J* 83: 290–298, 2002.

141. Sukharev S, Durell SR, and Guy HR. Structural models of the MscL gating mechanism. *Biophys J* 81: 917–936, 2001.

142. This reference has been deleted.

143. Sukharev SI, Blount P, Martinac B, and Kung C. Mechanosensitive channels of *Escherichia coli*: the MscL gene, protein, and activities. *Annu Rev Physiol* 59: 633–657, 1997.

144. Sukharev SI, Martinac B, Arshavsky, VY, and Kung C. Two types of mechanosensitive channels in the *E. coli* cell envelope: solubilization and functional reconstitution. *Biophys J* 65: 177–183, 1993.

145. Tang Y, Cao G, Chen X, Yoo J, Yethiraj A, and Cui Q. A finite element framework for studying the mechanical response of macromolecules: application to the gating of the mechanosensitive channel MscL. *Biophys J* 91: 1248–1263, 2006.

146. Tang Y, Yoo J, Yethiraj A, Cui Q, and Chen X. Gating mechanisms of mechanosensitive channels of large conductance, II: systematic study of conformational transitions. *Biophys J* 95: 581–596, 2008.

147. Thomas FC, Woeng C-A, Bloemberg GV, and Lugtenberg BJJ. Phenazines and their role in biocontrol by Pseudomonas bacteria. *New Phytologist* 157: 503–523, 2003.

148. Torchilin VP. Recent advances with liposomes as pharmaceutical carriers. *Nat Rev Drug Discov* 4: 145–160, 2005.

149. Tsai IJ, Liu ZW, Rayment J, Norman C, McKinley A, and Martinac B. The role of the periplasmic loop residue glutamine 65 for MscL mechanosensitivity. *Eur Biophys J* 34: 403–412, 2005.

150. Valadie H, Lacapcre JJ, Sanejouand YH, and Etchebest C. Dynamical properties of the MscL of *Escherichia coli*: a normal mode analysis. *J Mol Biol* 332: 657–674, 2003.

151. van den Bogaart G, Krasnikov V, and Poolman B. Dual-color fluorescence-burst analysis to probe protein efflux through the mechanosensitive channel MscL. *Biophys J* 92: 1233–1240, 2007.

152. Vasquez V, Cortes DM, Furukawa H, and Perozo E. An optimized purification and reconstitution method for the MscS channel: strategies for spectroscopical analysis. *Biochemistry* 46: 6766–6773, 2007.

153. Vasquez V, Sotomayor M, Cordero-Morales J, Schulten K, and Perozo E. A structural mechanism for MscS gating in lipid bilayers. *Science* 321: 1210–1214, 2008.

154. Vasquez V, Sotomayor M, Cortes DM, Roux B, Schulten K, and Perozo E. Three-dimensional architecture of membrane-embedded MscS in the closed conformation. *J Mol Biol* 378: 55–70, 2008.

155. Wang W, Black SS, Edwards MD, Miller S, Morrison EL, Bartlett W, Dong C, Naismith JH, and Booth IR. The structure of an open form of an *E. coli* mechanosensitive channel at 3.45 A resolution. *Science* 321: 1179–1183, 2008.

156. Wiggins P and Phillips R. Analytic models for mechanotransduction: gating a mechanosensitive channel. *Proc Natl Acad Sci U S A* 101: 4071–4076, 2004.

157. Wiggins P and Phillips R. Membrane-protein interactions in mechanosensitive channels. *Biophys J* 88: 880–902, 2005.

158. Wood JM. Osmosensing by bacteria: signals and membrane-based sensors. *Microbiol Mol Biol Rev* 63: 230–262, 1999.

159. Wood JN, Abrahamsen B, Baker MD, Boorman JD, Donier E, Drew LJ, Nassar MA, Okuse K, Seereeram A, Stirling CL, and Zhao J. Ion channel activities implicated in pathological pain. *Novartis Found Symp* 261: 32–40; discussion 40–54, 2004.

160. Wright JD and Higginson NAC. Effects of matrix variations on pH and Cu2 + sensing properties of sol–gel entrapped Eriochrome Cyanine R. *J Mater Chem* 14: 201–208, 2004.

161. Yang LM and Blount P. Manipulating the permeation of charged compounds through the MscL nanovalve. *FASEB J* 25: 428–434, 2011.

162. Yang LM, Wray R, Parker J, Wilson D, Duran RS, and Blount P. Three routes to modulate the pore size of the MscL channel/nanovalve. *ACS Nano* 6: 1134–1141, 2012.

163. Yang LM, Zhong D, and Blount P. Chimeras reveal a single lipid-interface residue that controls MscL channel kinetics as well as mechanosensitivity. *Cell Rep* 3: 520–527, 2013.

164. Yefimov S, van der Giessen E, Onck PR, and Marrink SJ. Mechanosensitive membrane channels in action. *Biophys J* 94: 2994–3002, 2008.

165. Yoshimura K, Batiza A, and Kung C. Chemically charging the pore constriction opens the mechanosensitive channel MscL. *Biophys J* 80: 2198–2206, 2001.

166. Yoshimura K, Batiza A, Schroeder M, Blount P, and Kung C. Hydrophilicity of a single residue within MscL correlates with increased channel mechanosensitivity. *Biophys J* 77: 1960–1972, 1999.

167. Yoshimura K, Usukura J, and Sokabe M. Gating-associated conformational changes in the mechanosensitive channel MscL. *Proc Natl Acad Sci U S A* 105: 4033–4038, 2008.

168. Zarychanski R, Schulz VP, Houston BL, Maksimova Y, Houston DS, Smith B, Rinehart J, and Gallagher PG. Mutations in the mechanotransduction protein PIEZO1 are associated with hereditary xerocytosis. *Blood* 120: 1908–1915, 2012.

169. This reference has been deleted.

170. Zhang X, Wang J, Feng Y, Ge J, Li W, Sun W, Iscla I, Yu J, Blount P, Li Y, and Yang M. Structure and molecular mechanism of an anion-selective mechanosensitive channel of small conductance. *Proc Natl Acad Sci U S A* 109: 18180–18185, 2012.

Address correspondence to:
Dr. Boris Martinac
Molecular Cardiology and Biophysics Division
Mechanosensory Biophysics Laboratory
Victor Chang Cardiac Research Institute
Darlinghurst
New South Wales 2010
Australia

E-mail: b.martinac@victorchang.edu.au

Abbreviations Used

3D structure = three-dimensional structure
CHO cells = Chinese hamster ovary cells
E. coli = *Escherichia coli*
ECR = Eriochrome cyanine R
EDTA = ethylenediaminetetraacetic acid
EPR = electronparamagnetic resonance
FLIM = fluorescence lifetime imaging
FRET = Förster resonance energy transfer
HEK-293 cells = human embryonic kidney cells
LPC = lysophosphatidylcholine
M. tuberculosis = *Mycobacterium tuberculosis*
MD = molecular dynamics
MS = mechanosensitive
MscCG = mechanosensitive channel of
Corynebacterium glutamicum

MscL = mechanosensitive channel of large
conductance
MscMJ = mechanosensitive channel of *Methanococcus
jannashii*
MscMJLR = mechanosensitive channel of *Methanococcus
jannashii* large and rectifying
MscS = mechanosensitive channel of small
conductance
MscSP = mechanosensitive channel of *Silicibacter
pomeroyi*
NiEdda = Ni(II)-ethylenediaminediacetate
S. aureus = *Staphylococcus aureus*
S. pombe = *Schizosaccharomyces pombe*
TREK-1 = member of the class of potassium channels
with two P domains related to TWIK-1
TWIK-1 = tandem of P domains in a weak inward
rectifier potassium channel